Impaired pituitary actions of thyrotropin-releasing hormone underlie central hypothyroidism in immunoglobulin superfamily, member 1 deficiency syndrome

By

Marc-Olivier Turgeon

Department of Anatomy and Cell Biology

Faculty of Medicine

McGill University

Montreal, QC, Canada

July 2016

Thesis submitted to McGill University in partial fulfillment of the requirements of the degree of Master's Science (MSc)

Dedicated to

My girlfriend and best friend, Lexi Stefanatos, who has supported me throughout this project and who is now (reluctantly) the savviest Art Historian on the topic of IGSF1.

And to my family, Dominique, Jean-François, Chloe, and Alex, who have always encouraged me to follow my passions and who bought me my first microscope.

Abstract

Loss-of-function mutations in the X-linked immunoglobulin superfamily, member 1 (*IGSF1*) gene cause central hypothyroidism. IGSF1 is a transmembrane glycoprotein of unknown function. It is expressed in thyroid-stimulating hormone (TSH) producing thyrotrope cells of the anterior pituitary gland. The protein is co-translationally cleaved into N- and C-terminal domains (NTD and CTD). The CTD is trafficked to the plasma membrane, whereas the NTD is retained in the endoplasmic reticulum (ER). Most intragenic *IGSF1* mutations in patients map to the CTD. To better understand IGSF1 function, we used the CRISPR-Cas9 system to introduce a loss-of-function mutation into the IGSF1-CTD in mice. The modified allele harbors a 312 bp deletion, removing part of exon 18 and intron 18. The resulting mRNA is expressed, though at greatly reduced levels relative to wild-type, and contains a novel hybrid exon. This exon introduces frame-shift and a premature stop codon, which affects the trafficking of the CTD. *Igsf1* deficient mice show normal serum TSH levels and normal numbers of TSH-expressing thyrotropes. However, expression of the TSH subunits, *Tshb* and *Cga*, and TSH protein content are reduced in these animals relative to wild-type littermates. Hypothalamic thyrotropin-releasing hormone (TRH) stimulates TSH synthesis and release. Importantly, pituitary TRH receptor (*Trhr)* mRNA levels are reduced in *Igsf1* deficient males. When challenged with exogenous TRH, *Igsf1* deficient mice release TSH, but to a significantly lesser extent than wild-type animals. The mice show similar impairments when endogenous TRH release is increased in response to reduced thyroid hormone feedback. Collectively, these results suggest that IGSF1 deficiency leads to central hypothyroidism via impairments in pituitary TRHR expression and/or downstream signaling.

Résumé

Les mutations causant une perte de fonction du gène membre 1 de la superfamille des immunoglobulines (*IGSF1*) qui se trouve sur le chromosome X, sont responsables d'un syndrome d'hypothyroïdie centrale. IGSF1 est une glycoprotéine transmembranaire ayant une fonction inconnue. Elle est exprimée dans les thyréotropes de l'hypophyse produisant la thyréostimuline (TSH). IGSF1 est clivées au moment de la traduction et se sépare en deux domaines: le domaine du terminal N (NTD) et du terminal C (CTD). Le CTD est transporté à la surface cellulaire tandis que le NTD est retenu dans le réticulum endoplasmique (ER). La majorité des mutations intra-géniques de *IGSF1*, découverte chez les patients, se trouvent dans la région qui encode le CTD. Pour mieux comprendre le rôle de IGSF1, nous avons utilisé le système CRISPR-Cas9 pour introduire une mutation causant une perte de fonction de IGSF1-CTD. L'allèle modifié contient une perte de 312 paires de bases qui engendre la perte d'une partie de l'exon 18 et de l'intron 18. L'ARN résultant est exprimé, malgré un niveau d'expression très bas comparativement aux souris de type sauvage, et contient un nouvel exon hybride. Cet exon introduit une mutation qui affecte le cadre the lecture de l'ARN, ce qui cause l'introduction d'un codon-stop prématuré, qui affecte le transport du CTD. Les souris déficientes en *Igsf1* démontrent des niveaux normaux de TSH en circulation ainsi qu'un nombre normal de thyréotropes produisant du TSH. Par contre, l'expression des différentes parties de TSH, *Tshb* and *Cga*, ainsi que le niveau de protéine de TSH contenu dans l'hypophyse sont réduits chez ces souris comparativement aux souris de type sauvage dans la même cage. L'hormone thyréostimuline (TRH) de l'hypothalamus stimule la synthèse et la sécrétion de TSH. Intéressement, l'ARNm des récepteurs de

TRH dans l'hypophyse (*Trhr*) est réduit chez les souris mâles déficientes en *Igsf1*. Quand ces souris sont stimulées avec une dose exogène de TRH, elles sécrètent du TSH, mais en quantité moindre que les souris de type sauvage. Les souris déficientes en *Igsf1* répondent semblablement à une hausse des niveaux de TRH endogène dû à une réduction des niveaux d'hormones thyroïde. Ensemble, ces résultats suggèrent qu'une déficience en IGSF1 engendre le syndrome d'hypothyroïdie centrale via une réduction de l'expression ou de la cascade de TRHR au niveau de l'hypophyse.

Table of contents

Figure list

Acknowledgements

I would like to thank my supervisor Dr. Daniel Bernard for his support and dedication to this project. Dr. Bernard has been a great mentor throughout my time in his lab, and I have learned so much from working with him. I will always look back on his strong work ethic and love of good science as an example to guide me in my future endeavors.

I would also like to acknowledge Dr. Mike Wade and thank him for his collaboration in working on this thesis. A thank you also goes to Dr. Kristen Vella for her expertise, specifically regarding the TRH stimulation assay, and for taking the time to discuss her ideas with me. This thesis would not be the same without their help and advice.

Thank you to all of the members of the Bernard lab for being such great lab mates and for always being ready to lend a hand. A special thank you to Dr. Luisina Ongaro for her help using the CRISPR-Cas9 gene editing methodology, and to Tanya Silander for first introducing me to the lab techniques and for teaching me the basics of doing research. I also want to thank Dr. Chirine Toufaily for her advice on cloning techniques and Xiang Zhou for her help with all of the animal work. Finally, to Yining Li, Gauthier Schang, and Ying Wang, thank you for your constant support. I have learned so much from each and every member of the lab and I will always remember my time here very fondly.

I also want to acknowledge the McGill transgenic core facility for assisting with the production of the new mouse model, and for performing cytoplasmic microinjections. Thank you to Severine Audusseau in the laboratory of Dr. Qutayba Hamid for her help

with the Luminex assay.

A thank you also goes to my committee members, Dr. Cheri Deal, Dr. John Bergeron, and my mentor, Dr. Alfredo Ribeiro-da-Silva, for their time and for their thoughtful discussions about my project.

Finally, thank you to all of the faculty and staff in the Department of Anatomy and Cell Biology and the Department of Pharmacology and Therapeutics.

The funding for the work presented in this thesis was provided by CIHR grant (MOP-133557) to Dr. Bernard, as well as CGS-M NSERC training grant and RQR-FONCER grant to the author.

Contributions of authors

T4 serum measurements were performed by Marc Rigden in the laboratory of Dr. Mike Wade (Health Canada) (Fig. 2.6C and 2.9B).

All other experiments, and the writing of this thesis, were conducted by the author under the supervision of Dr. Daniel Bernard.

Introduction

Control of thyroid hormone (TH) levels is important for metabolism (1-3), thermoregulation, (4) and development (5). Improperly low and high TH levels are clinically defined as hypothyroidism and hyperthyroidism, respectively. Hypothyroidism is characterized by decreased metabolism, which can lead to tiredness, dry skin, and shortness of breath among other symptoms (6, 7). Hyperthyroidism is marked by increased metabolism, fatigue, anxiety, palpitations, and heat intolerance among other characteristics (8). TH regulation is complex and there are, correspondingly, many causes of TH disorders.

In general, TH levels are controlled by the hypothalamic-pituitary-thyroid (HPT) axis (Fig. 1.1). Thyrotropin-releasing hormone (TRH) is released from TRH neurons of the hypothalamic paraventricular nucleus (PVN) into the pituitary portal vessels at the level of the median eminence (9, 10). TRH then binds to and activates TRH receptors (TRHR) expressed on thyrotrope cells in the anterior pituitary. TRHR activation stimulates transcription of the thyroid-stimulating hormone β gene (*Tshb*) (11, 12), and post-translational modification of the TSH protein (13). TSH is then released into the general circulation and acts on TSH receptors (TSHR) on thyroid gland follicular cells to stimulate the synthesis and release of the thyroid hormones triiodothyronine (T3) and thyroxine (T4). T3 and T4 have negative feedback effects at the level of the pituitary and on the TRH neurons (14-17). This model represents a relatively simple understanding of the HPT axis; there are, however, other regulatory mechanisms that render this axis far more complex. For example, THs require active transport into cells and can be metabolized locally into more or less active forms (18-22). Dysregulation of the HPT axis

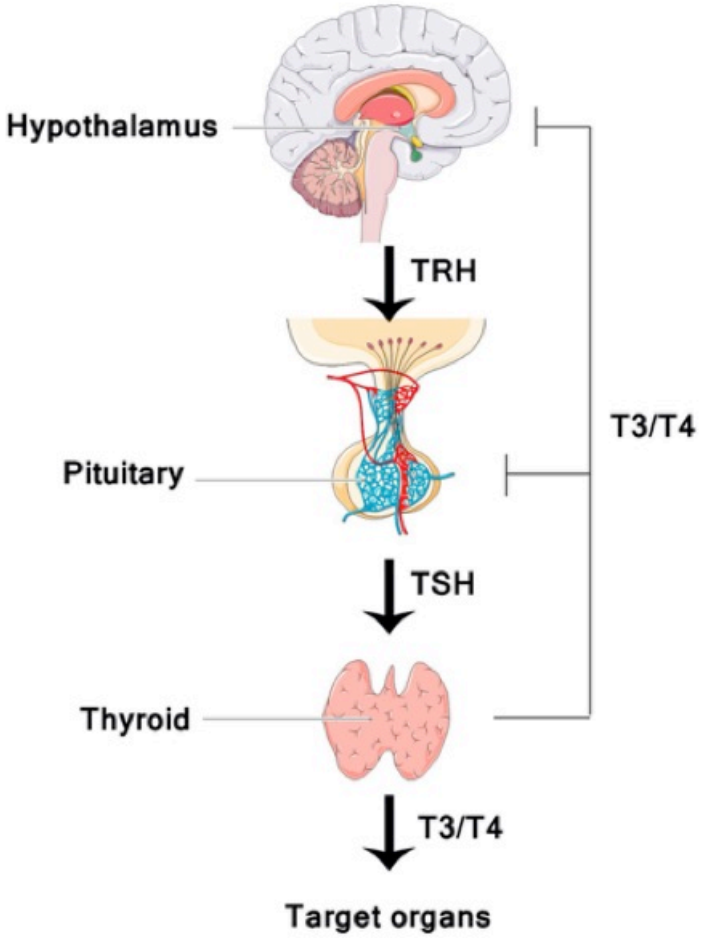

Figure 1.1 Hypothalamic-pituitary-thyroid axis. Diagram showing the basic regulation of thyroid hormone levels by the HPT axis. Thyrotropin-releasing hormone (TRH), thyroid stimulating hormone (TSH), triiodothyronine (T3), thyroxine (T4). Art is from Servier Medical Art.

at any level can lead to changes in TH levels and, therefore, to associated symptoms in patients. In this thesis, I focus on the mechanisms underlying a newly described form of central hypothyroidism. I first start with a more general discussion of different causes of hypothyroidism.

Primary hypothyroidism

The most common type of hypothyroidism, primary hypothyroidism, is characterized by a reduction in circulating TH levels due to a defect at the level of the thyroid gland (6), and occurs in 3.8-4.6% of the population (23). Affected patients show increased serum TSH levels due to the loss of THs negative feedback (24). However, the defective thyroid gland cannot respond appropriately to the increased TSH levels. One of the main causes of primary hypothyroidism worldwide is iodine deficiency (25). THs are formed from the precursor thyroglobulin, followed by the addition of covalently bound iodine groups to tyrosine residues (26). The number and location of iodine groups dictates the activity of thyroid hormones (24). The most active form of TH contains three iodine atoms and is called triiodothyronine (T3), while the less active form thyroxine (T4) contains four iodine groups. The 2 inactive forms of TH, diiodothyronine (T2) and reverse T3 (rT3), contain 2 and 3 iodine atoms respectively (27). Therefore, iodine insufficiency prevents the formation of active THs and leads to primary hypothyroidism. Patients with iodine deficiency often develop increases in thyroid gland size, known as goiter, due to the increased stimulation of the thyroid gland by high levels of circulating TSH.

Mutations in specific genes can also prevent the synthesis of functional THs from the thyroid gland. Follicular cells, or thyrocytes, of the thyroid gland are the cells that

produce thyroglobulin, T3 and T4. One of the key steps in the synthesis of T3 and T4 is the thyroperoxidase (TPO)-mediated oxidation of iodine, which is necessary for its covalent attachment to thyroglobulin (28). Therefore, mutations in *TPO* lead to a reduction in the synthesis of active THs and enlarged thyroid glands, which can be reduced to a normal size through T4 replacement therapy (29).

Other mutations found in human patients that lead to primary hypothyroidism include mutations in the *TSHR* gene. TSHR activation is not necessary for thyroglobulin production, however, it is necessary for the iodination of T3 and T4 hormones (26). Mice with inactivating mutations in the *Tshr* gene exhibit reduced T3 and T4 levels accompanied by an increase in TSH levels (26, 30). Mutations in the *TSHR* gene in humans impair the signaling of the TSHR (31). In one family, TSHR signaling is slightly impaired, resulting in increased pituitary TSH release to maintain normal TH levels in circulation (32).

Another major cause of primary hypothyroidism, which occurs in 0.3-1.2 % of the population, is Hashimoto's thyroiditis. It is the most prevalent cause of primary hypothyroidism in countries where iodine supplementation is sufficient in the population (33). It is an organ specific autoimmune disorder that results in lymphocyte infiltration in the thyroid and production of thyroid specific autoantibodies. Infiltrated immune cells impair thyroid function by inducing thyrocyte apoptosis, thereby reducing the production of thyroid hormones (34). Hashimoto's thyroiditis is caused by environmental factors as well as genetic predisposition. Specific mutations in the *thyroglobulin* and *TSHR* genes potentially increase chances of autoimmune reactions in thyrocytes. Mutations in genes in the immune system have also been linked with increased incidence of the disease (35).

Other possible causes of primary hypothyroidism include damage to the thyroid gland, either from drug treatment, tumors, or physical injury (trauma).

Central hypothyroidism

Central hypothyroidism (CH) is characterized by low thyroid hormone levels resulting from either low TSH circulating levels or normal levels of less bioactive TSH (36, 37). This can be caused by either a defect at the pituitary level (secondary hypothyroidism) or at the level of the hypothalamus (tertiary hypothyroidism). CH leads to similar, though generally less severe, symptoms as primary hypothyroidism (37). It most often occurs spontaneously due to injuries to the TSH producing cells in the pituitary or to the TRH neurons in the hypothalamus. Some examples include: pituitary adenoma, interruption of blood flow from the hypothalamus to the pituitary, surgery or radiotherapy, and/or other mass lesions (36-38). Other causes also include autoimmune diseases and/or infections that affect the hypothalamus or the pituitary. In these cases, CH can be transient if the underlying cause of the defect is addressed (37).

In addition to the spontaneous causes for CH, congenital mutations affecting pituitary cells can also result in this syndrome. Mutations in genes that encode transcription factors and signaling molecules important for pituitary development cause different pituitary hormone defects (39). For example, mutations in the transcription factors *HESX1, OTX2, PROP1, POU1F1, LHX3, LHX4, SOX2, SOX3*, and *GLI2* cause combined pituitary hormone deficiency (CPHD) to varying degrees (39, 40). CPHD is defined as improper production of two or more pituitary hormones. In some cases, it is also linked to other defects in, for example, the eyes or brain (39). These mutations and others that affect pituitary development can variably affect the differentiation and number

of thyrotropes (41). This leads to a reduction in TSH levels. CH is not the only symptom found in patients with CPHD, and it is often accompanied by reductions in growth hormone (GH), prolactin, and adrenocorticotropic hormone (ACTH) (40), which are produced by other pituitary cell types.

While mutations affecting the development of the pituitary can cause CPHD, congenital central hypothyroidism (CCH) can also be isolated and specific to thyrotropes. Mutations in the *TSHB* and *TRHR* genes, for example, have been described in patients with isolated CH. *TSHB* encodes for the beta subunit of TSH and provides for the biological specificity of TSH. The alpha subunit of TSH is encoded from the *CGA* gene and this subunit is common to TSH, luteinizing hormone (LH), and follicle stimulating hormone (FSH). Five different *TSHB* mutations have thus far been described (42, 43). These mutations cause low to normal levels of serum TSH with reduced levels of serum T4 (42-44).

Just like *TSHB* mutations, *TRHR* mutations also result in isolated CH in humans (45). The TRHR is a G-protein coupled receptor (GPCR) that signals mostly through the G proteins $G_{q/11}$ (Fig. 1.2) (46, 47). Upon TRH binding, $G_{q/11}$ activate the phospholipase C (PLC) pathway, resulting in increased intracellular calcium, activation of protein kinase C (PKC) (48-50), and mitogen-associated protein kinase (MAPK) signaling (51). TRH signaling activates a number of transcription factors, which regulate the expression of different genes including *TSHB*, *CGA*, and *TRHR* (12). TRH also regulates TSH glycosylation, which influences its biological activity (13). Few patients with biallelic deleterious *TRHR* mutations have been found (45, 52, 53). They express low to normal

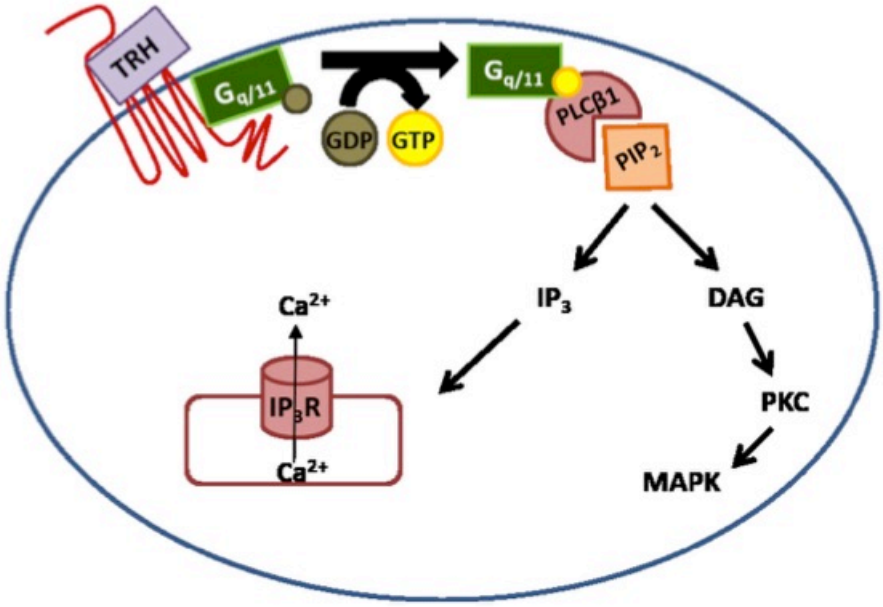

Figure 1.2 TRHR signaling pathway. Schematic representation of the molecular pathway activated by TRH binding to the TRHR. The TRHR is represented as red lines across the plasma membrane (blue circle). Modified from Tanya Silander, unpublished.

levels of serum TSH with reduced free T4 levels, consistent with a decrease in TSH production and/or bioactivity (45). The less bioactive forms of TSH are more stable in circulation than the more active forms, which could explain why the levels of serum TSH appear normal even though less TSH is produced (54, 55). *Trhr* knockout mice also exhibit reduced circulating levels of T3 and T4, with normal serum TSH levels, consistent with a less bioactive form of TSH (56).

IGSF1-deficiency syndrome

Recently, loss-of-function mutations in the immunoglobulin superfamily, member 1 (*IGSF1*) gene were discovered in approximately forty families with CCH (57-63). Mutations in *IGSF1* have an estimated prevalence of around 1:100,000 (58). *IGSF1* is located on the X chromosome, therefore, this syndrome primarily affects males. Patients exhibit CH with low to normal serum TSH levels and reduced free T4 levels. They also exhibit variable hypoprolactinemia and GH deficiency, as well as disharmonious pubertal development. That is, there is a delay in testosterone increase and development of secondary sexual characteristics, but normal timing of testicular growth. The testes continue to grow after the end of puberty and this leads to macroorchidism (enlarged testicles) in the adult males (57, 64). Patients with IGSF1-deficiency provide evidence that the IGSF1 protein plays an important, but previously unappreciated role in the regulation of the HPT axis. It has been suggested that IGSF1 may regulate TRHR signaling (59), however, more investigation is needed to confirm this idea and identify the underlying mechanisms.

IGSF1

The *IGSF1*/*Igsf1* gene encodes a 12 immunoglobulin (Ig; C2-type) loop

transmembrane glycoprotein (Fig. 1.3) (59, 65-67). IGSF1 is a member of the large and functionally diverse immunoglobulin superfamily (68). The IGSF1 protein is synthesized through the secretory pathway. It is co-translationally cleaved in the endoplasmic reticulum (ER) into N-terminal (NTD) and C-terminal (CTD) domains (Fig. 1.3). The CTD is expressed at the plasma membrane, whereas the NTD is retained in the ER (67). The CTD is a seven Ig-loop glycoprotein with a transmembrane domain and a short cytoplasmic tail (C-tail), while the NTD contains five Ig-loops with a transmembrane domain and a short C-tail. An additional transmembrane domain encoded by the *IGSF1* gene, which separates the NTD and CTD, is cleaved and degraded during the proteolytic cleavage in the ER (67) (Fig. 1.3).

IGSF1 is expressed in the anterior pituitary, choroid plexus, testes, and fetal liver (59, 69-71). In the pituitary, IGSF1 is specifically expressed in cell types of the so-called Pit1 lineages: thyrotropes, lactotropes, and somatotropes (59). IGSF1 is also expressed in the pituitary primordium, or Rathke's pouch, in mice, rats, and humans during development (59, 70). The murine *Igsf1* gene encodes at least four different mRNA isoforms in the pituitary. Isoform 1 (*Igsf1*-1) encodes the full-length protein; isoform 3 (*Igsf1*-3) encodes the whole NTD and the first 2 Ig-loops of the CTD; isoform 2 (*Igsf1*-2) encodes only for the first 2 Ig-loops of the NTD; and isoform 4 (*Igsf1*-4) encodes for the whole CTD (Fig. 1.4A) (69). The human *IGSF1* gene encodes at least five different mRNA isoforms. Isoforms 1, 3, and 4 (*IGSF1*-1, *IGSF1*-3, *IGSF1*-4) all encode the full-length protein, albeit with small variations due to alternative splice acceptor sites. Isoforms 2 and 5 (*IGSF1*-2, *IGSF1*-5) are identical in terms of coding sequence but differ in their 5' untranslated region, and encode the first two Ig-loops of the NTD similarly to

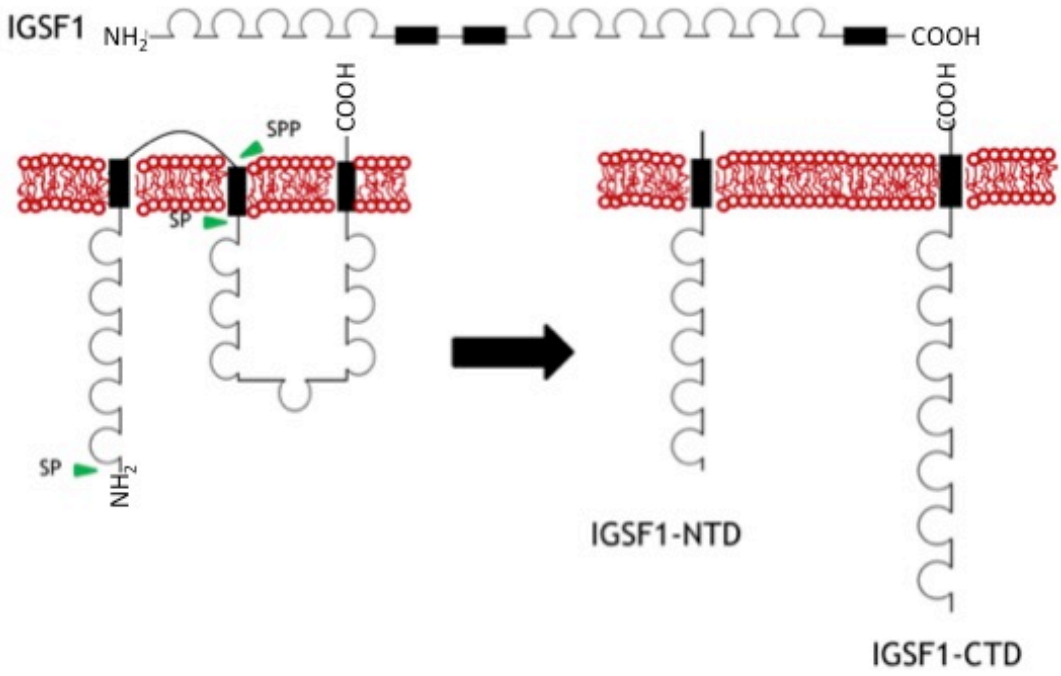

Figure 1.3 Proteolytic processing of IGSF1 in the ER. Schematic representation of IGSF1 cleavage that occurs in the ER. Representation of the full length IGSF1 protein (top), protein folded in the ER with cleavage sites (left), and a representation of the NTD and CTD fragments that result from the proteolytic processing (right). Transmembrane domains are represented by black boxes and Ig-loops are represented by semi-circles. Red lines represent the plasma membrane with the cytoplasm above, and the ER lumen below. Signal peptidase (SP), signal peptide peptidase (SPP). Modified from Tanya Silander, unpublished.

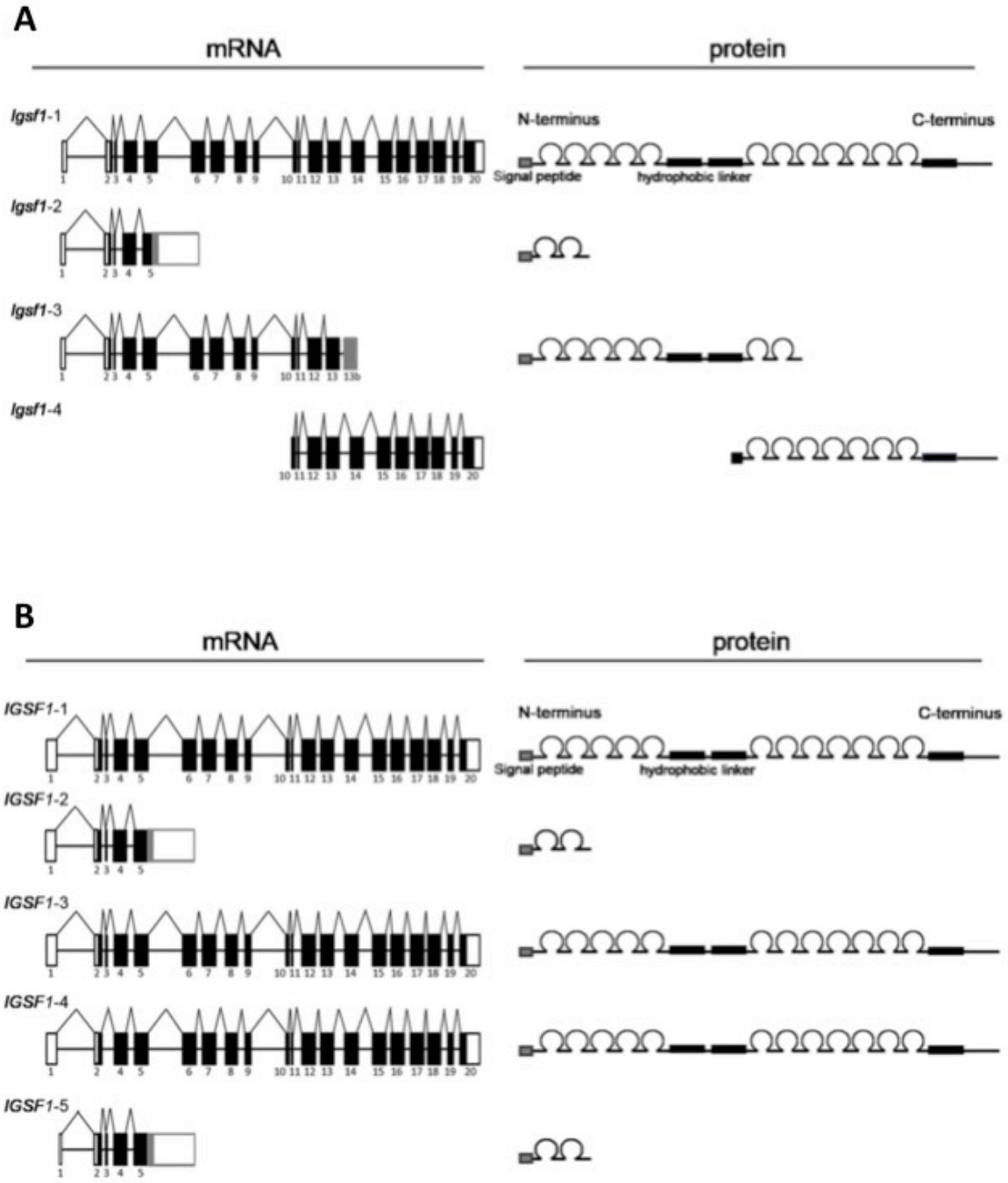

Figure 1.4 Mouse and human *Igsf1/IGSF1* isoforms. A) Schematic representation of the four mRNA isoforms of *Igsf1* expressed in mouse pituitary (left) with their corresponding encoded proteins (right). B) Schematic representation of the five different mRNA isoforms of *IGSF1* expressed in human (left) with their corresponding encoded proteins (right). On the mRNA side (left), black boxes represent translated exons, white boxes represent untranslated exons, and horizontal lines represent intron sequences. On the protein side (right), Ig-loops are pictured as semi-circles and transmembrane domains are shown as black boxes. Modified from Beata Bak, unpublished.

Igsf1-2 in mouse (Fig. 1.4B).

IGSF1 mutations

Mutations in *IGSF1* include whole gene deletions, frameshifts that prematurely truncate the protein (i.e., the CTD), and single amino acid substitutions. Interestingly, most mutations in *IGSF1* cluster in the part of the gene that encodes the CTD (Fig. 1.5). All of these mutations lead to a loss-of-function of IGSF1 and in most cases a loss of expression of IGSF1-CTD at the cell surface (59, 61-64, 72). The mutated forms of IGSF1-CTD are impaired in their glycosylation and trafficking and we suggest that they are trapped in the ER due to a misfolding of the protein. These trafficking defects suggest that expression of IGSF1-CTD at the cell surface is required for it to adequately fulfill its function. These findings, along with the fact that only IGSF1-CTD is expressed at the cell surface, support the hypothesis that IGSF1-CTD is the functional part of the protein.

Igsf1 knockout mice

An *Igsf1* knockout mouse model was previously designed by deleting exon 1 of the 20 exon *Igsf1* gene ($Igsf1^{\Delta ex1}$) (69). This model phenocopies the central hypothyroidism seen in IGSF1 deficient patients, however, the penetrance of the phenotype is variable (59, 69). These mice show low to normal serum TSH levels, with reduced pituitary TSH content, and low to normal serum T3 and T4 levels (T. Silander, unpublished) (59). While initial analysis in 2 cohorts of mice showed reduced T3 and T4 levels, subsequent experiments in different cohorts of mice reported normal circulating levels of the THs (T. Silander, unpublished) (59). This mouse model also exhibits an increase in pituitary GH content, as well as increased body weight compared to wild-type littermates (T. Silander and Y. Wang, unpublished) (59). There is, however, no change in

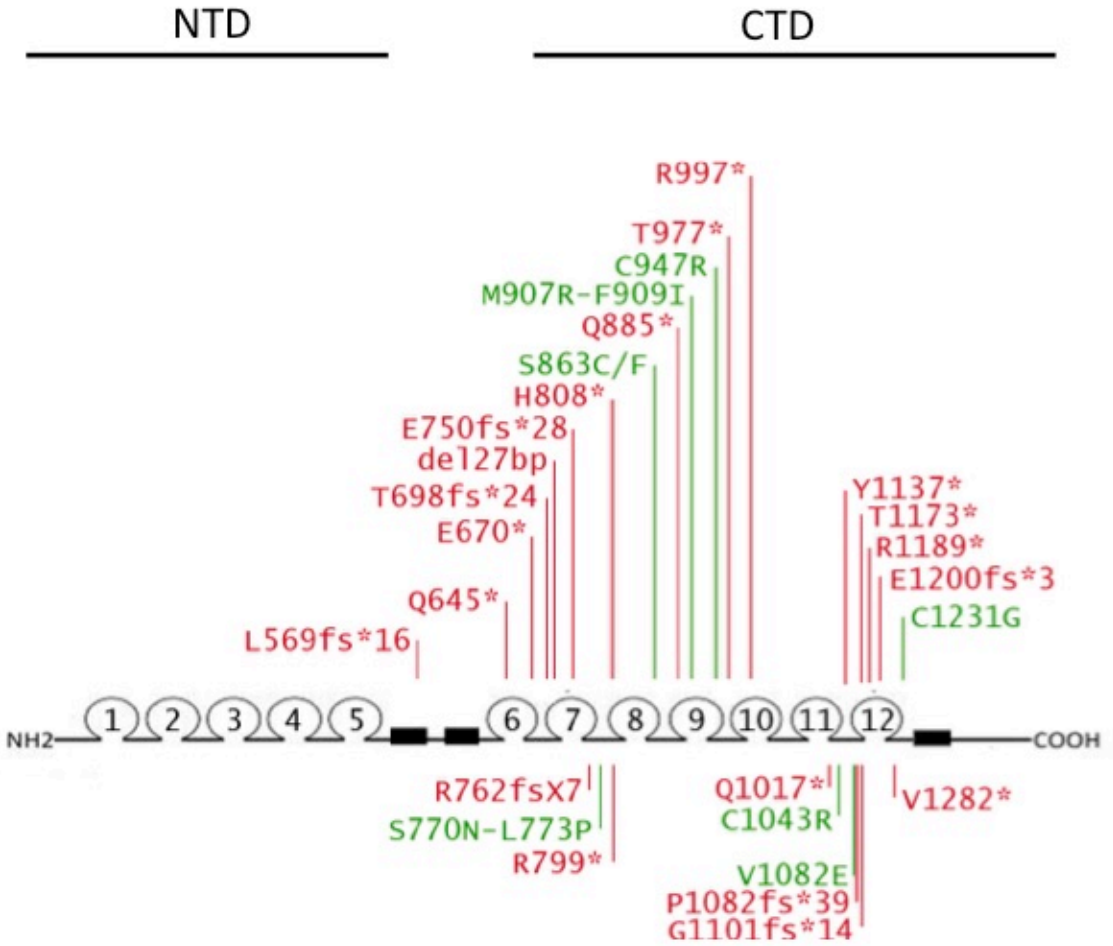

Figure 1.5 Schematic representation of the IGSF1 protein domain structure. The N-terminal and C-terminal domains (NTD and CTD) are labeled at the top. Ig loops are pictured as semi-circles and are numbered. Transmembrane helices are represented by black boxes. Pathogenic mutations discovered in patients are shown in red (indels and nonsense mutations) or green (missense mutations). Whole gene deletions are not shown.

testes weight or prolactin levels in *Igsf1*$^{\Delta ex1}$ mice.

One possible reason for the heterogeneity of the phenotype is that *Igsf1*$^{\Delta ex1}$ mice still express *Igsf1*-4. While a deletion of exon 1 effectively ablates pituitary *Igsf1*-1, *Igsf1*-2, and *Igsf1*-3, it does not prevent the expression of *Igsf1*-4 which derives from an intronic promoter in intron 9 of the *Igsf1* gene in mice (69). As mentioned above, *Igsf1*-4 encodes the entirety of the IGSF1-CTD. Despite the fact that *Igsf1*-4 is not upregulated in *Igsf1*$^{\Delta ex1}$ mice and that the protein it encodes has not been detected, it may still compensate for the loss of expression of some of the other *Igsf1* isoforms (67, 69). Another issue with the *Igsf1*$^{\Delta ex1}$ mice is that the deletion of exon 1 is not analogous to the mutations that are found in IGSF1 deficient patients.

Aims of thesis

As mentioned above, we hypothesize that IGSF1 might be involved in TRHR signaling and that mutations in IGSF1 could cause an impairment in this pathway. In this thesis, I test this hypothesis and investigate further the role of IGSF1 in the regulation of the HPT axis. More specifically, I aim to address the potential shortcomings of the current *Igsf1*$^{\Delta ex1}$ mouse model by developing a new mouse model that disrupts the functional part of IGSF1 (i.e., the CTD). This will allow us to: 1) create a mutation more analogous to those found in IGSF1-deficient patients, and 2) to disrupt IGSF1-CTD derived from any mRNAs containing exons 10-20 of *Igsf1*. This new mouse model expresses a similar phenotype compared to the *Igsf1*$^{\Delta ex1}$ mice. Interestingly, all Igsf1-deficient mice exhibited blunted TSH release following endogenous or exogenous increases in TRH. Taken together, these data suggest a role for IGSF1 in TRHR signaling.

Materials and methods

CRISPR guide RNA

DNA oligonucleotides encoding the CRISPR RNA (crRNA) sequence were purchased from IDT (Coralville, IA) (sense: 5' – CACCGGCTCCACAACA GTTTTCCG – 3', antisense: 5' – AAACCGGAAAACTGTTGTGGAGCC – 3'). The oligos were annealed and 5' phosphorylated in the same reaction. Briefly, 10 μM of each primer were mixed with 1X T4 ligase buffer (Promega, Madison, WI), and 5 U of T4 polynucleotide kinase (New England Biolabs, Whitby, Ontario) and incubated at 37°C for 30 min. The reaction was then incubated at 95°C for 5 min before the temperature was ramped down to 25°C at a rate of 5°C/min. The annealed oligos were ligated into the pX330 vector (# 42230, Addgene, Cambridge, MA) in a digestion-ligation reaction. Briefly, the pX330 vector was digested with 10 U of *Bbs*I (FastDigest, ThermoFisher, Burlington, Ontario), while, in the same reaction, the oligos were ligated into the digested vector using 10 U of T4 DNA ligase (Promega) in the presence of 1X FastDigest buffer, 1 mM DTT, and 1 mM ATP. The reaction was cycled 6 times for 5 min at 37°C and 5 min at 23°C. The resulting plasmid (11 μl) was treated with 10 U of PlasmidSafe exonuclease (Epicentre, Madison, WI) in the presence of 1X PlasmidSafe buffer and 1 mM ATP at 37°C for 30 min, and transformed into NEB10 competent bacteria. Single colonies were selected and grown in 3 ml cultures of lysogeny broth. Plasmid DNA was extracted using a plasmid DNA extraction kit (BioBasic, BS614, Markham, Ontario) and confirmed by Sanger sequencing (Genome Québec, Montreal, Quebec). Part of the plasmid including the T7 promoter and gRNA, which comprises crRNA and transactivating CRISPR RNA (tracrRNA), were amplified by PCR using oligos from IDT

(sense: 5’ – TAATACGACTCACTATAGGCTCCACAACAGTTTTCCG – 3’, antisense: 5’ – AAAAGCACCGACTCGGTGCC – 3’). The PCR product was gel-purified with the BioBasic gel extraction kit (BS654) following the manufacturer’s instructions, and transcribed to RNA using the MAXIscript T7 kit (AM1312, ThermoFisher, Burlington, Ontario) following manufacturer’s instructions.

Development of new *Igsf1* deficient mice

Mice were generated by cytoplasmic microinjections of the gRNA described above and *Cas9* mRNA (Sigma, CAS9MRNA, Oakville, Ontario) into single cell mouse C57BL6/N zygotes. The microinjections were performed at the Goodman Cancer Research Centre Mouse Transgenic Facility. The injected zygotes were cultured overnight in KSOM (Zenith Biotech, ZEKS-050, Guilford, Connecticut) droplets under mineral oil (Zenith Biotech, ZSCO-100) in a 35 mm dish at 37°C in a 5% CO_2 incubator. The 36 embryos that developed to the 2-cell stage were transferred to the oviducts of 2 pseudopregnant CD1 females. Five pups were born and were genotyped by PCR amplifying from genomic DNA extracted from tail biopsies using 0.5 ml of lysis buffer [100 mM Tris-HCl (pH 8.5), 5 mM EDTA (pH 8.0), 200 mM NaCl, 0.2% (v/v) SDS, and 100 μg/ml proteinase K]. The targeted region of *Igsf1* was amplified by PCR using the following primers (sense: 5’ – GGGTGACTGGTAAGGTTCTG – 3’, reverse: 5’ – CAACAGGCCCTGTGGTATATC – 3’), resolved on a 1% agarose gel, and gel-purified. The product was sent for direct Sanger sequencing (Genome Québec) using the following primers (5’ – GACATCACCCTTCAGTGCCG – 3’, 5’ – CAGGCTGAGTC cCTCAGATCTCC – 3’). A founder female had 6 bp and 312 bp deletions in her two *Igsf1* alleles, both of which were germline transmissible. As described in the Results, the

312 bp mutation, subsequently called *Igsf1*$^{\Delta 312}$, was pursued. Off-target mutations were assessed by amplifying genomic regions where potential mutations could occur using primers in Table 1. The PCR product were then sent for sequencing using the sense primers shown in Table 1.

Animal housing and collection

All animals were housed on a 12L:12D light:dark cycle and were given *ad libitum* access to food and water. The diet consisted of standard rodent chow (2020X, Teklad diets, Envigo, Toronto, Ontario) unless otherwise specified. Eight to 10-week-old animals were euthanized by CO_2 asphyxiation. Blood was collected by cardiac puncture, and pituitary glands were extracted and either flash frozen in liquid nitrogen, or frozen in liquid nitrogen in 500 µl of TRIzol. All animal work was conducted in accordance with federal and institutional guidelines and with the approval of the Goodman Cancer Centre Facility Animal Care Committee at McGill University (protocol #5204).

Constructs

Plasmid encoding the pcDNA3 vector was purchased from Invitrogen. The IGSF1-4 construct was generated by Thalia Robakis. Briefly, cDNA encoding the CTD of murine *Igsf1* was obtained from ATCC (clone number: 3289361). The sequence was amplified with primers containing *BamH*I and *Not*I sites and ligated into the pNice vector (Dr. Peter Scheiffele) using those restriction enzyme sites. The IGSF1-4-HA, IGSF1-4-Δ6bp, and IGSF1-4-Δ9bp construct were derived from the IGSF1-4. The N-terminal HA tag was added to IGSF1-4 by reverse PCR amplification of the IGSF1-4 plasmid with phosphorylated primers (sense: 5' – GATTACGCTATCGATGCATTGACAGA GGAGATTGAAATAGTCATGCC – 3', antisense: 5' – TGGAACATCGTATGG

Gene	Sense primer	Antisense primer
NM_001033548	5' – TTTCTCGCTGCCCCGCTTCT – 3'	5' – TCTCCAGCTCCCAGCTCCA – 3'
NM_011122	5' – CTAAACAGGCCTCACCGTG – 3'	5' – AGAAGACCCGCGCTTGGTC – 3'
NM_033622	5' – TGTCGTCTCCGTTGCGTGAA – 3'	5' – CTGCTAAACAGTGTGGCTTGTC – 3'
Chromosome 2	5' – GAGCTTCAGTGCAGTATTGC – 3'	5' – GCCTACAGTCACTTTGACTC – 3'
Chromosome 4	5' – CACTGACAGCACCATCACAG – 3'	5' – GGCACACTTACAGCTCCCAT – 3'
Chromosome 11	5' – TTGGCAGACCTTGGTCGTGT – 3'	5' – TGCCTGAATGCCTGGTTCCT – 3'

Table 1. List of primers used to amplify potential sites for off-target mutations.

GTATGCCCCATTGCACAGTCCACAGCA – 3') following the QuickChange mutagenesis cycling conditions. The resulting linear PCR product was ligated back together with 10 U of T4 DNA ligase at 4°C overnight. The 6 and 9 bp deletions were introduced using the QuickChange mutagenesis protocol with the following primers (6 bp deletion, sense: 5' – CCACAACAGGAGGATGGAGATTTTGTCATCGAC AACTTGGA – 3', antisense: 5' – TCCATCCTCCTGTTGTGGAGCCTCTTCTCCA TCATGCTCTA – 3'; 9 bp deletion, sense: 5' – CCACAACAGGATGG AGATTTTGTCATCGACAACTTGGAAGG – 3', antisense: 5' – ATCTCCATCCTG TTGTGGAGCCTCTTCTCCATCATGCTCTA – 3'). All plasmids were transformed into NEB10 competent bacteria and confirmed by sequencing (Genome Quebec).

Cell transfection

HEK293 cells (provided by Dr. Terry Hébert, McGill University) were cultured in Dulbecco's Modified Eagle Medium (DMEM, 319-005Cl, Wisent inc., Saint-Jean-Baptiste, Quebec) supplemented with 10% fetal bovine serum (FBS, 12483-020, Gibco, Burlington, Ontario). The cells were seeded at 800,000 cells per well in 6-well plates (3516, Costar, Corning, New York), and were transfected with the indicated plasmid the following day. Two µg of plasmid were incubated in serum-free DMEM with 6 µg of polyethylenimine (PEI) for 15 min. The complex was then added to the cells in serum-free medium and incubated for 2 h, before the medium was changed to complete medium.

Immunoblotting and deglycosylation assays

SDS-PAGE, immunoblots, and protein extraction were performed essentially as in Sun et al. (59). Briefly, for lysates from tissue, pituitary glands were dissected from 8-week-old males, immediately frozen in liquid nitrogen, and kept at -80 °C until analysis.

The protein lysates were extracted by adding 50-100 µl of RIPA buffer [150 mM NaCl, 50 mM sodium fluoride, 10 mM $NaPO_4$, 2 mM EDTA, 1% NP-40, 1% sodium deoxycholate, 0.1% SDS] directly in the tube containing the frozen tissue. A handheld homogenizer was used to dissociate the tissue. To extract lysates from cell culture, cells were washed 2 times with 1 ml of PBS and then incubated for 20 min with 300 µl IP lysis buffer [50 mM Tris (pH 7.5), 150 mM NaCl, 1 mM EDTA, 1% Triton X-100]. The cells were then transferred to 1.5 ml tubes. Lysates from cells and pituitaries were sonicated with a microtip probe sonicator (Sonicator 3000, Misonix) for 15 sec at 3 Watts and then spun down for 20 min at 13,000 rpm at 4°C. Protein concentrations were measured using BCA assays (ThermoFisher) following the manufacturer's instructions. Where indicated, 20 µg of protein lysates were denatured at 95°C for 10 min and then deglycosylated with 50 U of EndoH, PNGaseF,(P0702S, P0704S, New England Biolabs) or left untreated for 2 h at 37°C prior to being resolved by SDS-PAGE. In all other cases, 10 µg of protein lysates were denatured at 70°C for 10 min in Laemmli buffer and resolved by SDS-PAGE on 8% Tris-glycine gels. Proteins were transferred to Protran nitrocellulose membranes (NBA083C001EA, Perkin Elmer, Waltham, MA), blocked in 5% nonfat milk in Tris-buffered saline [TBS; 150 mM NaCl, 10 mM Tris (pH 8.0)] containing 0.05% Tween 20 (TBST), and incubated in the indicated primary antibody in 5% milk in TBST overnight at 4°C with agitation. The rabbit anti-mouse IGSF1 primary antibody was first described in Robakis et al. (1:1000) (67), and the mouse anti-β-actin antibody was purchased from Sigma Aldrich (1:40000, A5441, St-Louis, Missouri). The next day, the membranes were washed in TBST and subsequently incubated in HRP-conjugated rabbit or mouse secondary antibody (1:5000, goat anti-mouse 170-6516, goat anti-rabbit 170-

6515, BioRad, Mississauga, Ontario) in 5% milk in TBST. Blots were washed in TBST, incubated with ECL Western Lightning Plus (NEL105001EA, Perkin-Elmer, Boston, Massachusetts), and exposed to HyBlot CL Autoradiography film (E3018, Denville Scientific Inc., Metuchen, New Jersey).

TRH stimulation

Adult male *Igsf1*$^{+/y}$ and *Igsf1*$^{\Delta 312/y}$ mice were injected with TRH (P1319, Sigma-Aldrich, 10 μg/kg of body weight) by i.p. injection of around 200 μl of 1 ng/μl of TRH diluted in phosphate buffer saline (PBS) containing 0.002% BSA. Half of the mice were injected at 8 weeks and the other half were injected at 9 weeks. Prior to injection, blood was collected from the tail vein by creating a small incision with a scalpel on either side of the tail, around 1.5 to 3 cm from the base. Thirty μl of blood was collected using EDTA-coated microvettes (20.1278.100, Sarstedt, Nümbrecht, Germany) and immediately kept on ice. Blood samples were also collected 15 min, 1 h, and 2 h following TRH injection by rubbing the scab off of the previous incision with a sterile gauze soaked in PBS and proceeding as with the first sample. The samples were spun at 3,000 rpm for 10 minutes at 4°C and the plasma was collected and stored at -20°C until analyzed. To minimize stress, the mice were handled daily for 2 weeks prior to the experiment and were not restrained during blood collection.

Diet-induced hypothyroidism

Ten-week-old mice were fed a low iodine diet supplemented with 0.15% propylthiouracil (LoI/PTU, TD.95125, Teklad diets, Envigo, Toronto, Ontario) for 3 weeks *ad libitum*. The diet was changed every Monday, Wednesday, and Friday to replace the PTU. Blood samples were collected from the animals prior to starting the diet,

and after 1 week and 2 weeks on the diet, by performing submandibular venipuncture (~100-200 µl). At the end of the third week, the animals were sacrificed, their blood was collected by cardiac puncture (~500-800 µl), and their pituitary glands were collected in 500 µl of TRIzol (Invitrogen, Burlington, Ontario) and immediately frozen in liquid nitrogen. Serum was collected from the blood samples as described above.

Hormone measurements

T4 levels were measured using a commercially available ELISA kit purchased from MP Biomedicals (Cat# 07BC-1007, Cedarlane, Burlington, Ontario) following the manufacturer's instructions. The measurements were carried out by Marc Rigden in the laboratory of Dr. Mike Wade at Health Canada (Ottawa, Ontario). The data were collected using a SpectraMax Plus 384 (Molecular Devices) plate reader and analyzed using SoftMax Pro V 5.0.1. The range of detection was between 0.5 to 25 µg/dl. The intrassay coefficient of variation (CV) was 1.4%, and the interassay CV was 6.8%. TSH levels in *Igsf1*$^{\Delta 312/y}$ mice were measured using the MILLIPLEX MAP mouse pituitary magnetic bead panel from EMD Millipore (MPTMAG-49K, Darmstadt, Germany) following the manufacturer's instructions. The serum samples collected during the LoI/PTU diet experiment were diluted 1:5 in serum matrix provided in the kit prior to measurement, as pilot experiments indicated that undiluted samples from animals on the diet were out of the assay range. Ten µl of the dilutions were used in the assays. Protein lysates were extracted from frozen pituitary glands to measure TSH content using lysis buffer [50 mM HEPES, 150 mM NaCl, 10 mM EDTA, 1% (v/v) Triton X-100, 1 mM Na_3NO_4, 30 mM NaF, 10 mM $Na_4P_2O_7$, 1 µg/ml pepstatin A, 1 µg/ml leupeptin, 1 µg/ml aprotinin, 1mM PMSF], and diluted 1:10,000 in assay buffer included in the kit. Ten µl of

the dilutions were used in the assay. The MAGPIX instrument with XPONENT software was used for the measurements and the analysis was performed using the MILLIPLEX Analyst 5.1 software. The range of detection was between 12.21 to 50,000 pg/ml. The intrassay CV was 2.68%, and the interassay CV was 4.38%.

RT-qPCR

RNA was extracted from frozen pituitary glands in TRIzol following the manufacturer's instructions. Briefly, pituitary glands were homogenized for 30 sec in 500 µl of TRIzol using a Polytron PT 10-35 homogenizer, and 100 µl of chloroform was added. The aqueous layer containing RNA was collected, and 250 µl of isopropanol was added to precipitate the RNA. The pelleted RNA was washed two times with 500 µl of 70% ethanol before being dissolved in 20 µl RNase/DNase free water. Some of the resulting RNA (100 ng) was treated with 1 U RQ1 DNase (M6101, Promega, Madison, WI) and reverse transcribed with 100 U M-MLV RT enzyme (M170B, Promega) in the presence of 20 U of RNAsin (N2111, Promega). Two µl of the resulting cDNA was analyzed per reaction by qPCR with the EvaGreen 2X qPCR MasterMix-S from Applied Biological Materials Inc. (ABM, Richmond, British-Columbia), and 0.4 pmol of *Tshb*, *Trhr*, *Cga*, *Igsf1*, *Gh*, *Prl*, *Lhb*, *Fshb*, or *Rpl19* primers (Table 2). The reactions were performed on a Corbett Rotor-Gene 6200 HRM (Corbett Life Science) according to the EvaGreen cycling conditions. Each sample was run in duplicate, and normalized to *Rpl19* using the $2^{-\Delta\Delta Ct}$ method (73).

3' RACE

RNA was extracted from pituitaries as described above. One µg of RNA was reverse transcribed with reagents in the FirstChoice RLM-RACE kit from Ambion (AM1700,

Gene	Sense primer	Antisense primer
Tshb	5' – GAACGGTGGAAATACCAGGA – 3'	5' – AGAAAGACTGCGGCTTGGTGCA – 3'
Cga	5' – TCCCTCAAAAAGTCCAGAGC – 3'	5' – GAAGAGAATGAAGAATATGCAG – 3'
Trhr	5' – CTCCCCAACATAACCGACAG – 3'	5' – GCAGAGAAACTGGGCTTTGA – 3'
Gh	5' – ACCTCGGACCGTGTCTATGA – 3'	5' – GCAGCCCATAGTTTTTGAGC – 3'
Prl	5' – AAGCAGCTTCTTGAGGGAGTT – 3'	5' – TGTTGCGCAAAGACAAGATT – 3'
Fshb	5' – GTGCGGGCTACTGCTACACT – 3'	5' – CAGGCAATCTTACGGTCTCG – 3'
Lhb	5' – AGCAGCCGGCAGTACTCGGA – 3'	5' – ACTGTGCCGGCCTGTCAACG – 3'
Rpl19	5' – CGGGAATCCAAGAAGATTGA – 3'	5' – TTCAGCTTGTGGATCTGCTC – 3'
Igsf1	5' – TGAGTTGGGTCAAGAGGATT – 3'	5' – TGAGGAGTTACCAGGATAGAGGA – 3'
Igsf1^{+}	5' – CCTGATATCTGGTCAGAGCC – 3'	5' – CCACAATCAGGGTACTTCGG – 3'
Igsf1$^{\Delta 312}$	5' – CTGCCAGGAGTTGAATTTGTG – 3'	5' – GCTGAGTCACTCAGATCTCC – 3'

Table 2. List of primers used for qPCR analysis of gene expression.

ThermoFisher). Gene specific primers (outer: GAGATCTGGGTGACTGGTAAG, inner: GATAAGCTTCCTAAA CCCTCTCTGTCAGCC) were used with the kit's outer and inner primers, respectively, to amplify the region of interest by nested PCR. The inner PCR product, flanked with *BamH*I and *Hind*III restriction digest site, was ligated into pBluescript II KS (+) (X52328, Stratagene, La Jolla, CA) digested with *BamH*I and *Hind*III using 10 U of T4 DNA ligase in the presence of 1X T4 DNA ligase buffer at 4°C overnight. The plasmid was transformed into NEB10 competent bacteria, white colonies were selected, and the plasmid DNA was extracted and sequenced (Genome Québec).

Immunohistochemistry

Mice were injected with TRH (10 µg/kg of body weight) as described above. Thirty min following TRH injections, the mice were injected with an overdose of Avertin (20 µl/g of body weight, T48402, Sigma Aldrich) followed by isofluorane inhalation. The anesthetized mice were then perfused intracardially with 20 ml of PBS, followed by 20 ml of 4% paraformaldehyde (PFA) in PBS. The pituitary glands were dissected and fixed further in 4% PFA in PBS for 1 h at RT, followed by an overnight incubation in a 30% sucrose solution in PBS. The pituitary glands were frozen in OCT compound (4583, Tissue-Tek, Sakura Finetek, Torrance, California), sectioned at 5 µm with a Leica cryostat, and mounted on glass slides. The sections were washed with PBS containing 0.5% Triton X-100. They were then incubated with 0.5% hydrogen peroxide (H_2O_2) solution in PBS for 30 min at RT. Following three 10 min washes in PBS, the sections were blocked for 1 h at RT in 3% normal donkey serum in PBS and incubated overnight at RT with a rabbit c-Fos antibody (1:8000, ABE157, EMD Millipore). The next day, the sections were washed in PBS, incubated with goat anti-rabbit biotinylated secondary

antibody (1:200, BA-1000, Vector laboratories, Burlingame, California) in 3% donkey serum for 1 hour at RT, washed 3 times for 10 min in PBS, incubated with Vectastain ABC reagents for 30 min at RT (PK6100, Vector laboratories), and washed 3 times for 10 min in PBS again. The sections were then incubated in a 3,3'-diaminobenzidine (DAB) solution with nickel sulfate ($NiSO_4$) [0.05% DAB, 0.05% $NiSO_4$, 0.015% H_2O_2, in PBS (pH 7.2)] for 5 min, followed by washing 3 times for 10 min in PBS. The sections were then incubated in goat anti-TSHβ antibody (1:500, sc-7815, Santa Cruz, Dallas, Texas) overnight at RT. The same steps as above were repeated but using rabbit anti-goat biotinylated secondary antibody (1:200, BA-5000, Vector laboratories) as the secondary antibody, and omitting the $NiSO_4$ from the DAB solution. Coverslips were then mounted using Permount. Sections were examined using a Leica DM 1000 LED microscope. The $TSH\beta^+$ cells (i.e., brown cells) and the $TSH\beta^+$/c-Fos^+ cells (i.e., brown cells with black nuclei) were counted in 2 sections per animal. For each section, the number of $TSH\beta^+$ cells was normalized to the size of the area counted. The $TSH\beta^+$/c-Fos^+ cells are expressed as a percentage of total $TSH\beta^+$ cells for each section.

Statistical Analyses

Body weight, testis weight, and hormone measurements were compared using unpaired t-tests. Statistical comparisons of mRNA levels were made using unpaired t-tests, with Welch's correction when the standard deviations were significantly different as assessed by F-test. The mRNA levels from *Igsf1*$^{\Delta 312/y}$ animals were normalized relative to the levels of *Igsf1*$^{+/y}$ littermates for each gene analyzed. In the case of the mRNA analysis of the mice on the normal and LoI/PTU diets, *Tshb*, *Cga*, and *Trhr* data were transformed by square root transformation to make the distributions normal. Data from

TRH injection experiments with the *Igsf1*$^{\Delta 312/y}$ mice were analyzed by 2-way ANOVA. The data from the LoI/PTU diet experiment with *Igsf1*$^{\Delta 312/y}$ mice were analyzed with a hybrid repeated measures 2-way ANOVA. Genotype was a between-subject factor, and time was a within-subject factor. The TSH levels after 3 weeks on the diet and 15 min post-TRH injections were also compared by unpaired t-tests post-hoc. Data from the IHC quantitation were analyzed by 2-way ANOVA. The number of replicates and results of the statistical tests are found in the text and figure legends. The statistical analyses were made using GraphPad Prism 6. Significance was assessed relative to $p < 0.05$.

Results

Generation of a novel *Igsf1* loss of function mouse model

We previously reported that *Igsf1*$^{\Delta ex1}$ mice are centrally hypothyroid (59). A concern with this model, however, is that the mice continue to express the *Igsf1*-4 mRNA isoform (69). *Igsf1*-4 encodes the entirety of the IGSF1-CTD (B. Bak, unpublished) and therefore could at least partially compensate for the loss of the protein derived from the larger, more abundant *Igsf1*-1 transcript. Although *Igsf1*-4 is not upregulated in pituitaries of *Igsf1*$^{\Delta ex1/y}$ mice (69), the variable penetrance of the hypothyroid phenotype raises concerns about compensation, at least in some animals. To address this concern, we generated a new loss-of-function mouse model that directly affects the CTD, regardless of the transcript from which it is derived.

There are no consensus mutations in IGSF1 deficient patients, however, there is a relatively high density of frame-shift and nonsense mutations in exon 18, which encodes the terminal 12th Ig loop. We therefore used CRISPR-Cas9 technology to introduce deletions in *Igsf1* exon 18 of one-cell murine zygotes (74, 75). We caused a site-specific Cas9 cleavage that resulted in a double-strand break repaired by the error-prone DNA repair machinery (74, 75). An initial litter of five pups contained one male and one female without any observable *Igsf1* mutations (CRISPR.1 and CRISPR.5 in Fig. 2.2); one male with a 9 bp deletion (recall that *Igsf1* is X-linked; CRISPR.3); one female with a 6 bp deletion on one allele and no mutation on the other (CRISPR.4); and a female (hereafter CRISPR.2) with a 6 bp deletion on one allele and a 312 bp deletion on the other (Fig. 2.1, 2.2A, lane 1).

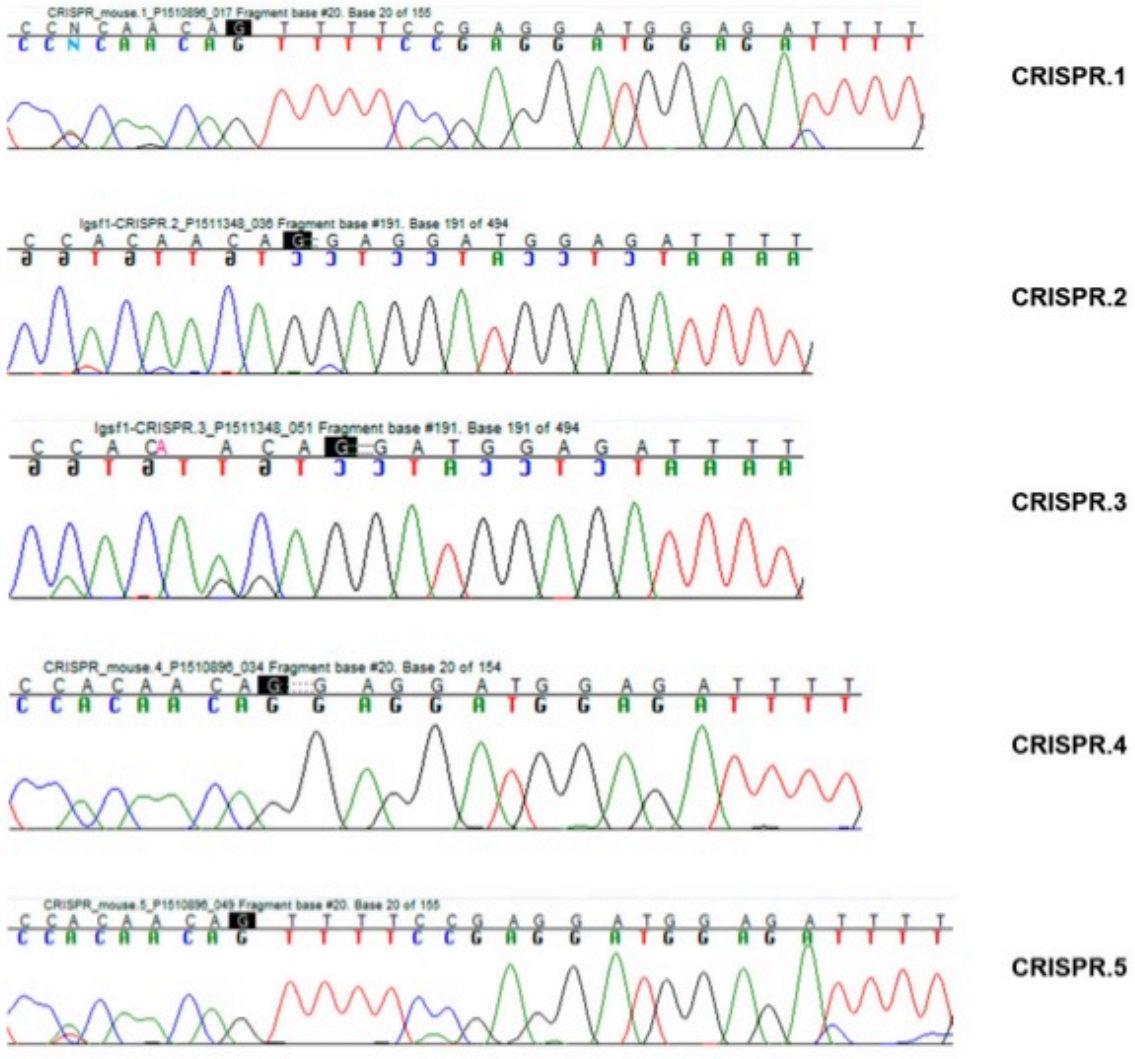

Figure 2.1 Genomic DNA sequence of original founder animals. Chromatograms of direct Sanger sequencing of exon 18 of the *Igsf1* gene of the 5 founder mice. The nucleotides highlighted in black show the site of the Cas9 cleavage. ":" represent deleted nucleotides.

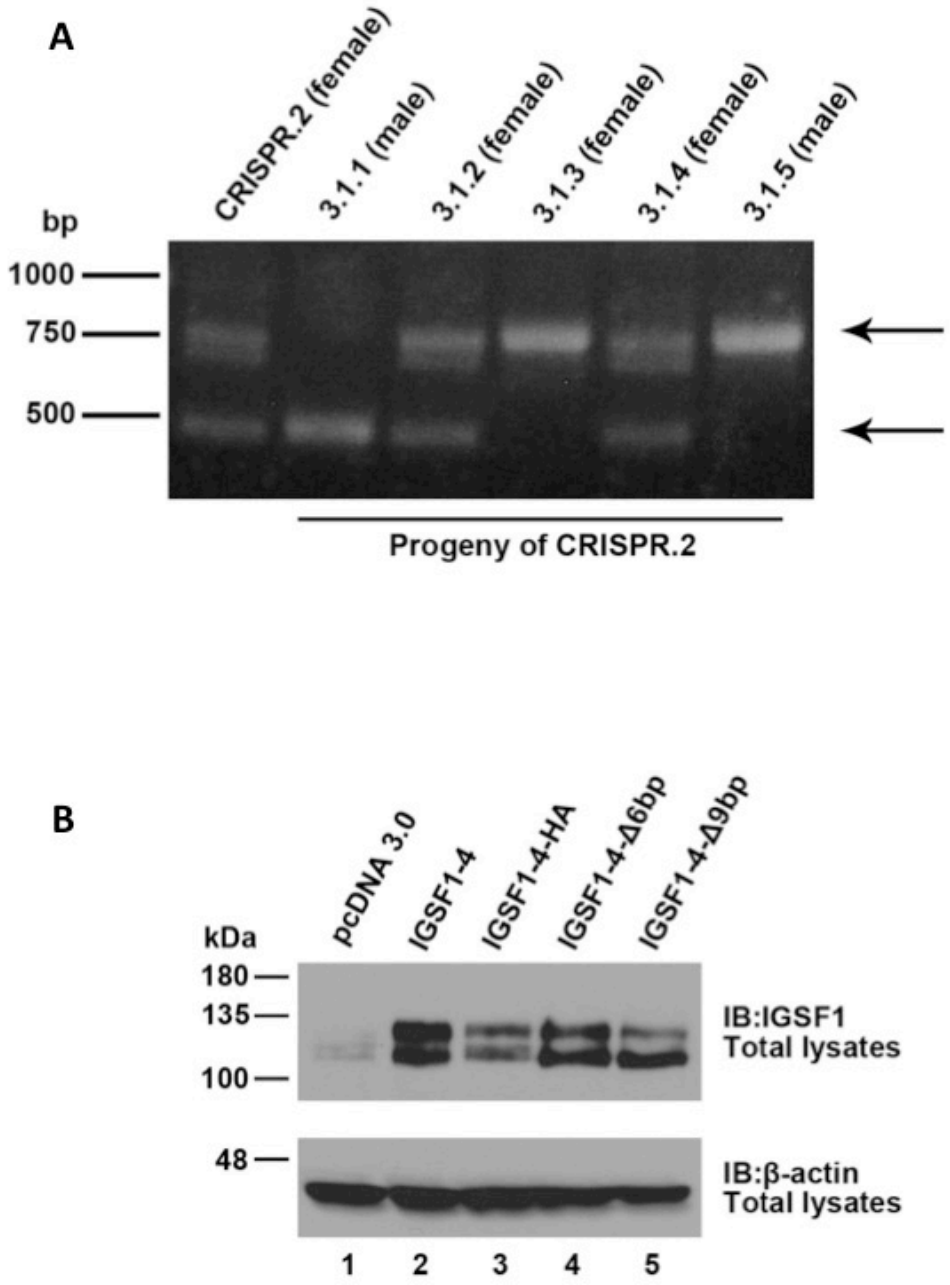

Figure 2.2 *Igsf1* deletions resulting from the CRISPR-Cas9 design. A) PCR amplification of the targeted region in exon 18 of *Igsf1* in the founder female (CRISPR.2, lane 1) and five of her progeny (3.1.1.-3.1.5, lanes 2-6). Arrows at the right indicate the wild-type (top) or Δ312 (bottom) alleles. B) Western blot of HEK293 cells transfected with expression vectors encoding different forms of the murine IGSF1-CTD, derived from the *Igsf1*-4 cDNA. The blot was probed with a rabbit anti-mouse IGSF1-CTD antibody (top) and then mouse anti-β actin (bottom). Lane 1: empty vector. Lane 2: untagged IGSF1-4. Lane 3: IGSF1-4 with three C-terminal HA tags. Lane 4: IGSF1-4-HA with the 6 bp deletion. Lane 5: IGSF1-4-HA with the 9 bp deletion.

As the 6 and 9 bp deletions were in-frame, we examined whether they were damaging in a heterologous *in vitro* expression system. Neither deletion markedly affected expression of the IGSF1-CTD (Fig. 2.2B, lane 4 and 5). In contrast, the 312 bp deletion encompassed the 3' end of exon 18 (139 bp) and the 5' end of intron 18 (173 bp) of the *Igsf1* gene (Fig. 2.3A, right panel). This deletion, which we now refer to as *Igsf1*$^{\Delta 312}$, was predicted to cause a frame-shift and premature termination of the CTD (more below). We therefore pursued analyses using this allele.

The 312 bp deletion allele encodes a truncated IGSF1-CTD

The *Igsf1* mRNA transcript was altered in pituitaries of *Igsf1*$^{\Delta 312}$ males (note, as this is an X-linked gene and a male-specific disorder, our analysis was limited to male mice). In contrast to the splicing of exons 18 and 19 seen in wild-type mice, the mutants expressed an mRNA harboring a novel hybrid exon comprising the 5' end of exon 18 (140 bp) and the 3' end of intron 18 (215 bp) spliced to exon 19 (Fig. 2.3A). As a result, 47 amino acids from exon 18 were lost and 6 novel amino acids were added from the retained intron 18 sequence, before the introduction of a premature stop codon. Amino acids encoded by exons 19 and 20, including the transmembrane domain and intracellular C-tail, were lost (Fig. 2.3B). No *Igsf1*$^{\Delta 312}$ mutants expressed the wild-type mRNA (Fig. 2.3C) and no wild-type mice expressed the mutant mRNA in their pituitary glands (Fig. 2.3D).

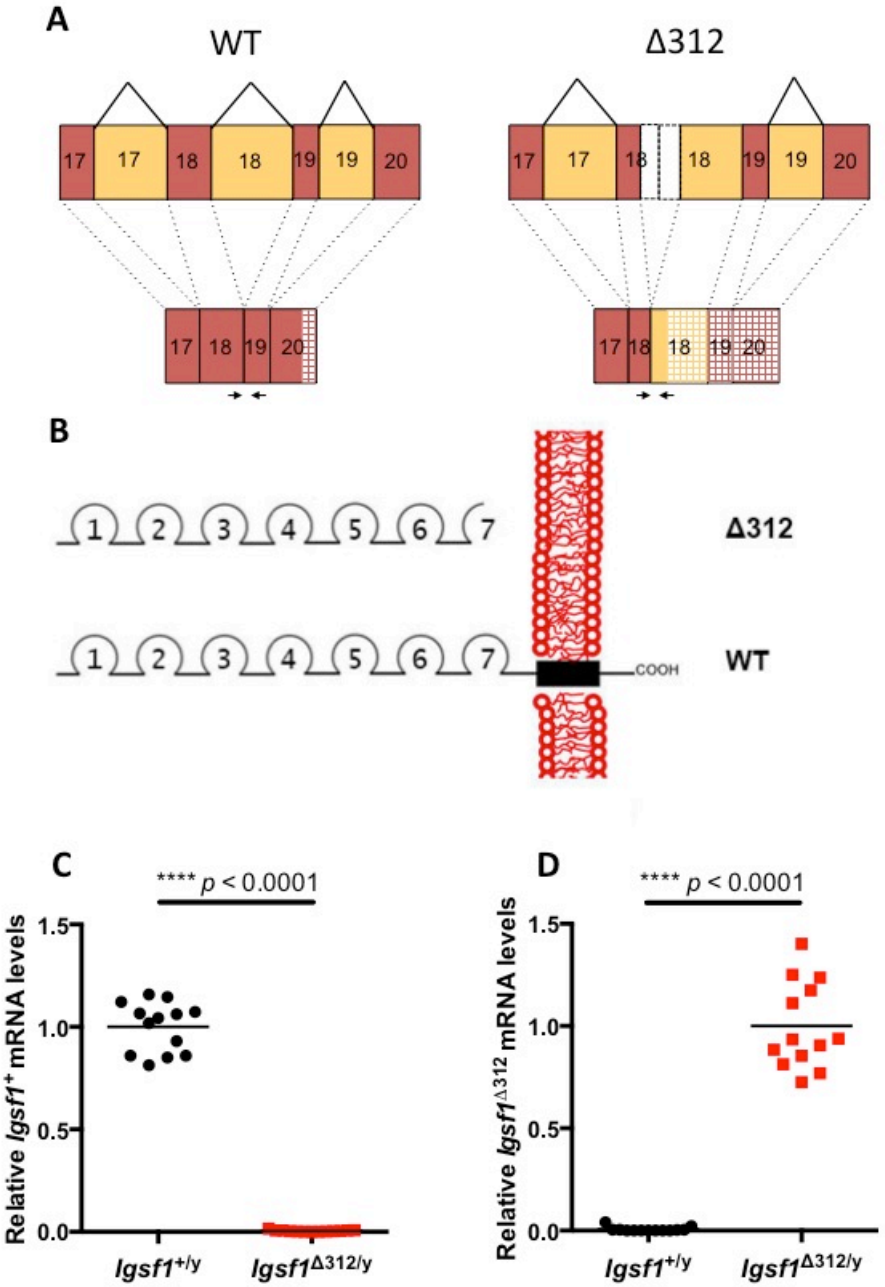

Figure 2.3 Generation of *Igsf1* loss-of-function mice. A) Genomic organization and RNA splicing around exons 17-20 of the wild-type (left) and Δ312 alleles (right). Exons are presented as red boxes and are numbered. Intervening introns are shown as yellow boxes. The deleted parts of exon 18 and intron 18 in the Δ312 allele (right) are pictured at the top with stippled lines. The part of the intron 18 that is retained in the transcript derived from this allele is shown in yellow. Grid pattern is used to represent untranslated mRNA. B) Schematic representation of the IGSF1-CTD protein derived from the wild-type (WT) and Δ312 alleles. C-D) RNA was extracted from pituitaries of adult wild-type (black circles) or Δ312 males (red squares). mRNA expression of *Igsf1* (WT transcript only) (C) and *Igsf1* (Δ312 transcript only) (D) was analyzed by RT-qPCR. Group means are indicated with solid horizontal lines. Arrows in (A) represent the primers specific to each genotype that were used in the RT-qPCR. The data were analyzed by two-tailed t-tests, C) ($t = 29.42$, $df = 12.03$, **** $p < 0.0001$), D) ($t = 16.89$, $df = 12.07$, **** $p < 0.0001$).

Premature truncation of the human protein in Ig loop 12 prevents membrane trafficking of the IGSF1-CTD (59, 61, 63, 76, 77). This appeared to be the case in *Igsf1*$^{\Delta 312}$ mice as well. The IGSF1-CTD in wild-type mouse pituitary migrated as a doublet on SDS-PAGE (Fig. 2.4A, lanes 1-4). These represent mature (top band; EndoH-resistant) and immature glycoforms (bottom band; EndoH-sensitive) of the protein (Fig. 2.4B, lanes 2 and 5). In contrast, neither of these protein glycoforms was expressed in pituitaries of *Igsf1*$^{\Delta 312}$ males (Fig. 2.4A, lanes 5-10). Rather, they expressed a novel, truncated protein of about 90 kDa. This protein was EndoH-sensitive (Fig. 2.4B, lanes 8 and 11), indicating that it was a glycoprotein that failed to transit from the ER to the Golgi.

IGSF1-CTD protein expression in pituitaries of *Igsf1*$^{\Delta 312}$ mice was reduced relative to wild-type (Fig. 2.4A and B). Though we did not rule out an effect on protein stability, lower abundance protein expression derived, at least in part, from markedly reduced *Igsf1* mRNA expression or stability in *Igsf1*$^{\Delta 312}$ mice (Fig. 2.4C).

To address concerns about off-target effects of the Cas9 enzyme, we examined the three non-coding and three coding regions most likely to be targeted by the gRNA, according to Hsu et al. (78). None of these regions were altered in *Igsf1*$^{\Delta 312/y}$ mice (Fig. 2.5).

Igsf1$^{\Delta 312}$ mice exhibit central hypothyroidism on a control diet

Having established the loss of IGSF1 protein expression and trafficking in pituitaries of *Igsf1*$^{\Delta 312}$ males, we next characterized their phenotypes. Adult *Igsf1*$^{\Delta 312}$ males had significant increased body mass compared to their wild-type littermates (Fig. 2.6A), consistent with what we reported previously in *Igsf1*$^{\Delta ex1}$ mice (59). In contrast to

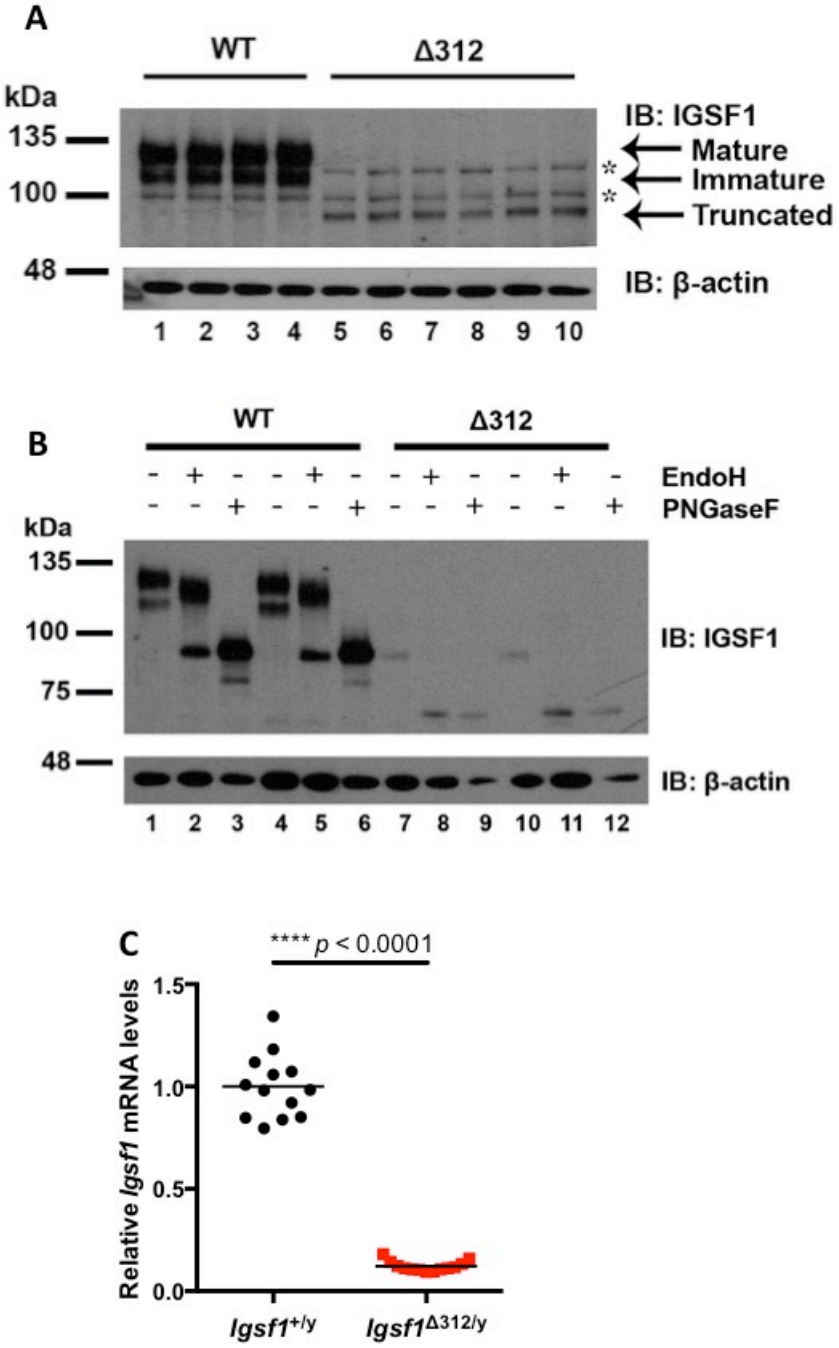

Figure 2.4 Reduced IGSF1 protein and mRNA expression in *Igsf1*$^{\Delta 312}$ mice. A) Proteins extracted from individual adult wild-type (lanes 1-4) and Δ312 males (lanes 5-10) were subjected to SDS-PAGE and western blotting using an anti-IGSF1-CTD antibody. Arrows mark the mature and immature glycoforms in wild-type and the truncated protein in Δ312 males. *, non-specific bands. B) Protein extracts from two wild-type (lanes 1-6) and two Δ312 males (lanes 7-12) were treated with EndoH or PNGaseF prior to western analysis as in panel A. C) RNA was extracted from pituitaries of adult wild-type (black circles) or Δ312 males (red squares). mRNA expression of *Igsf1* was analyzed by RT-qPCR. Group means are indicated with solid horizontal lines. The data were analyzed by two-tailed t-test, ($t = 19.95$, $df = 12.64$, **** $p < 0.0001$).

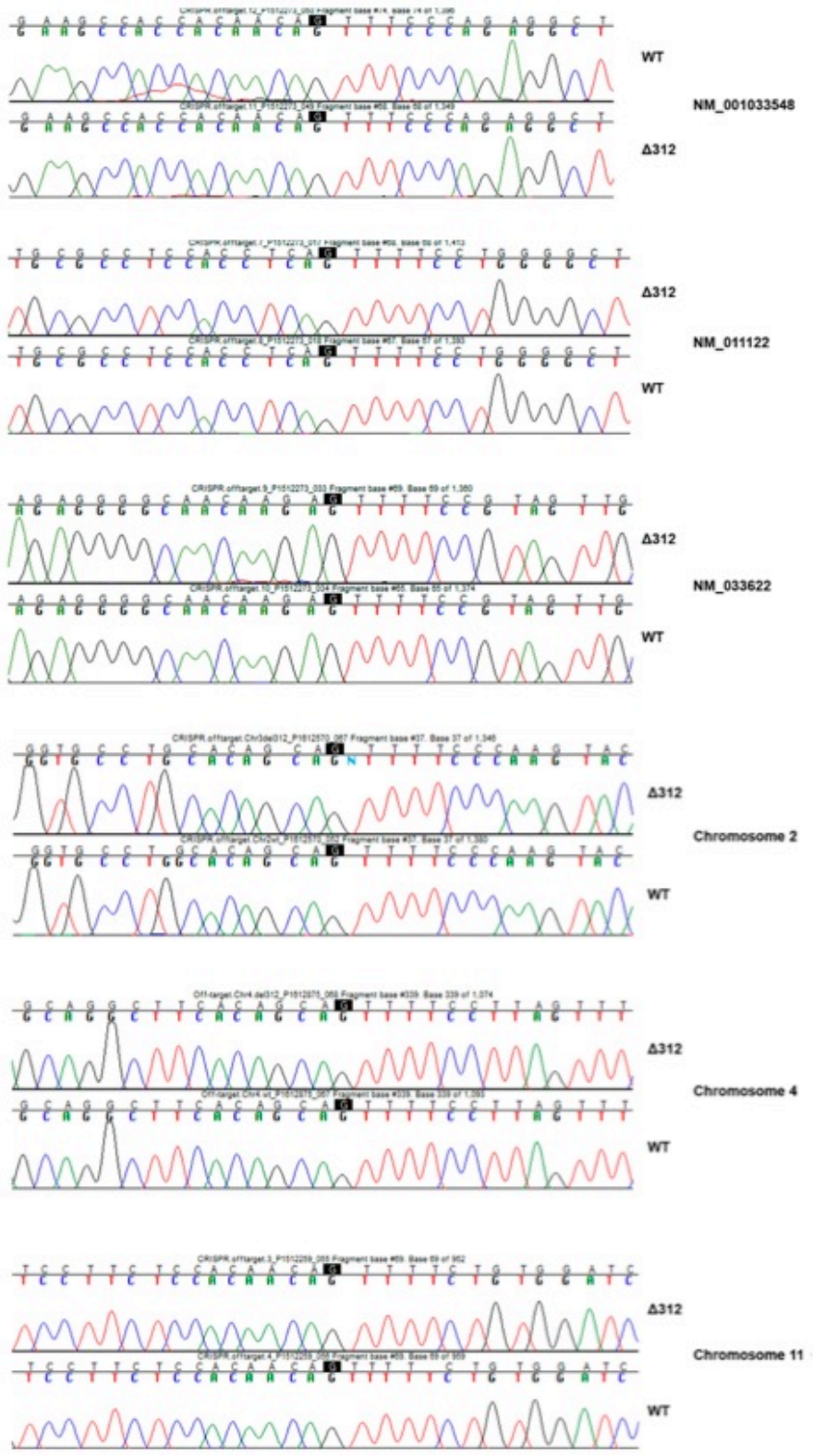

Figure 2.5 Sequence of potential off-target sites. Chromatograms of direct Sanger sequencing of amplified genomic regions where there are possibly off-target mutations. The sequence of Δ equ males compared to wild-type males are shown. The highlighted nucleotides represent the potential Cas9 cleavage site.

Igsf1$^{\Delta ex1}$ mice, however, *Igsf1*$^{\Delta 312}$ males had increased testis mass, even when correcting for the difference in body mass (Fig. 2.6B).

We previously reported that *Igsf1*$^{\Delta ex1}$ males had suppressed TSH and T3 levels on a control diet relative to wild-type (59). Follow-up analyses in the same strain yielded variable results, with TSH, T4, and T3 levels differing or not between genotypes depending on the experiment (Tanya Silander, unpublished). Here, serum TSH and T4 levels were statistically equivalent between *Igsf1*$^{\Delta 312/y}$ males and their wild-type littermates (Fig. 2.6C and D), though there was a non-significant trend for TSH levels to be reduced in the former. Remarkably, there were significant decreases in pituitary mRNA levels for *Tshb*, *Cga*, and *Trhr* in the same *Igsf1*$^{\Delta 312/y}$ males relative to wild-type (Fig. 2.7A-C). *Gh* but not *Prl*, *Fshb*, or *Lhb* mRNA levels were increased in pituitaries of *Igsf1*$^{\Delta 312/y}$ relative to wild-type males (Fig. 2.7D-G). In light of these results, we measured pituitary hormone content for both TSH and GH in a second cohort of animals. TSH levels were reduced (Fig. 2.8A) and GH levels had a non-significant trend to be increased (Fig. 2.8B) in pituitaries of *Igsf1*$^{\Delta 312/y}$ relative to wild-type males. Notably, serum TSH again showed the non-significant trend for reduced levels in *Igsf1*$^{\Delta 312}$ males relative to controls in this second cohort. Serum GH was not measured given the requirement for serial blood sampling to accurately measure this hormone.

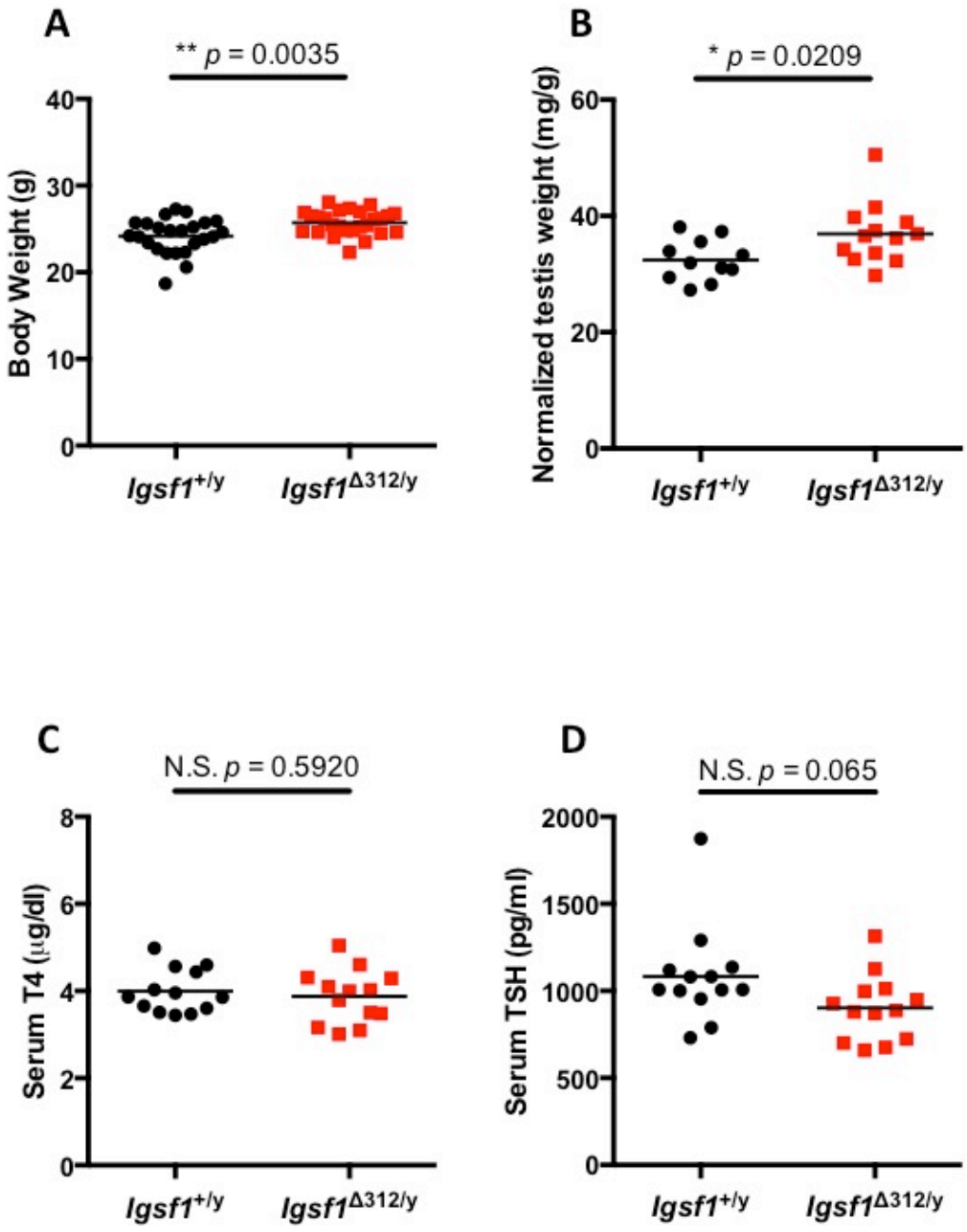

Figure 2.6 Body weight and testis weight are increased in Δ312 males compared to wild-type, while serum TSH and T4 levels are unchanged. (A) Body weight and (B) testis weight normalized to body weight, from 8-week-old wild-type and *Igsf1*$^{\Delta 312/y}$ males. Serum (C) T4 and (D) TSH levels in another cohort of 10-week-old wild-type and *Igsf1*$^{\Delta 312}$ males. The data were analyzed by two-tailed t-tests: A) t = 2.940, df = 24, ** p = 0.0072, B) t = 2.496, df = 21.14, * p = 0.0209, C) t = 0.5435, df = 23.04, N.S. p = 0.5920, D) t = 1.946, df = 21.16, N.S. p = 0.0651.

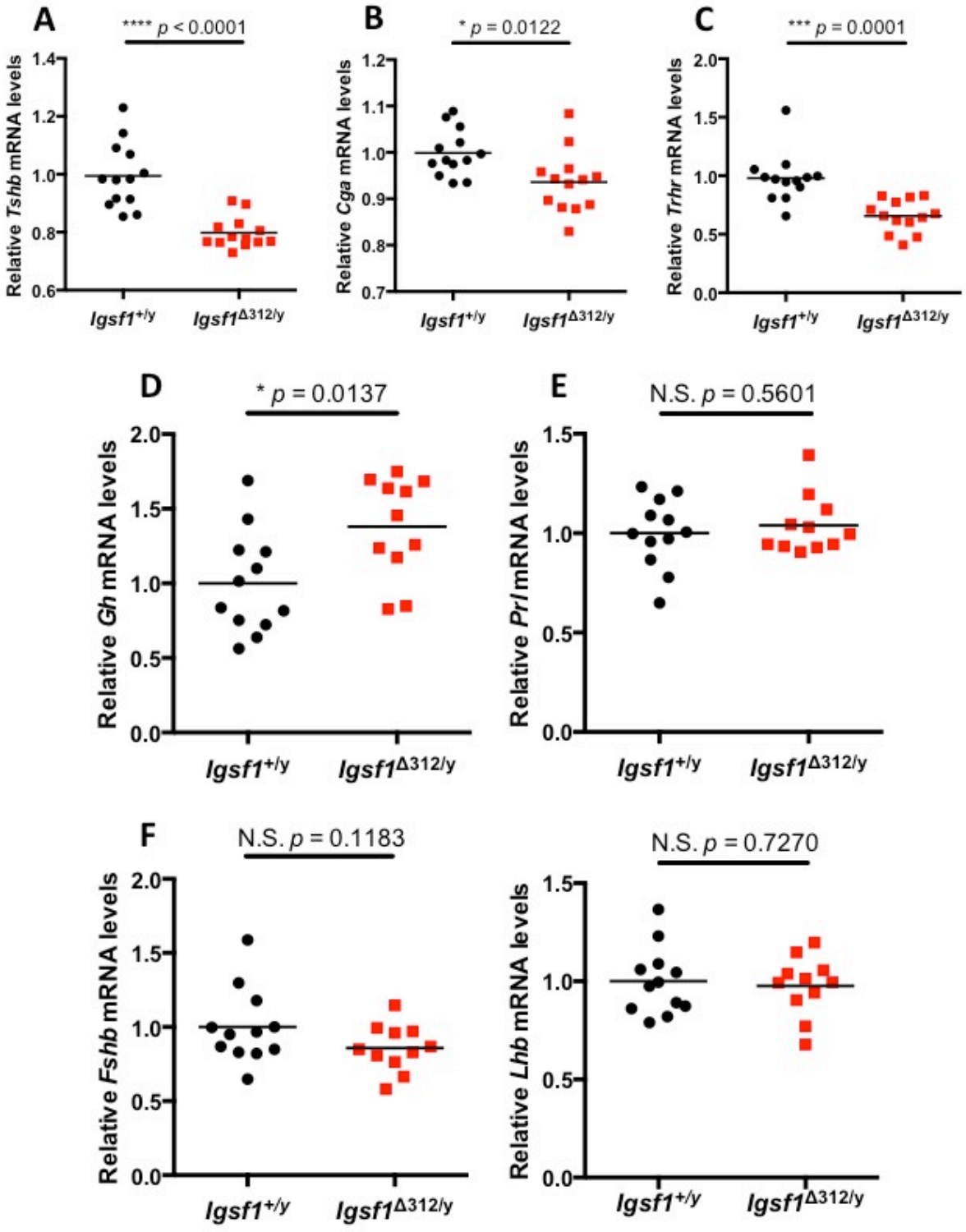

Figure 2.7 HPT axis function is altered in *Igsf1*$^{\Delta 312}$ mice. A-G) *Tshb*, *Cga, Trhr*, *Gh*, *Prl*, *Fshb*, and *Lhb* mRNA levels in pituitaries of 10-week-old wild-type and *Igsf1*$^{\Delta 312/y}$ males. The data were analyzed by two tailed t-tests, A) t = 5.6666, df = 17.13, **** $p < 0.0001$, B) t = 2.727, df = 22.40, * $p = 0.0122$, C) t = 4.651, df = 20.83, *** $p = 0.0001$, D) t = 2.692, df = 20.90, * $p = 0.0137$, E) t = 0.5922, df = 20.88, N.S. $p = 0.5601$, F) t = 1.637, df = 18.75, N.S. $p = 0.1183$, G) t = 0.3539, df = 20.97, N.S. $p = 0.7270$.

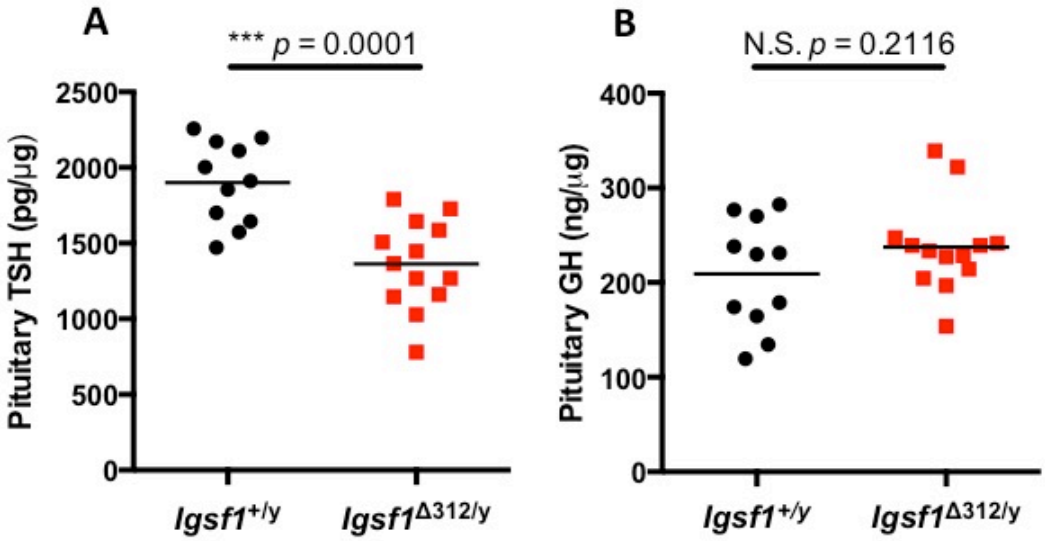

Figure 2.8 TSH protein content is lower in *Igsf1*$^{\Delta 312/y}$ compared to *Igsf1*$^{+/y}$ mice. Pituitary (A) TSH and (B) GH protein content in 10-week-old wild-type and *Igsf1*$^{\Delta 312\ /y}$ males. The data were analyzed by two-tailed t-tests, A) t = 4.645, df = 21.78, *** p = 0.0001, B) t = 1.291, df = 19.68, N.S. p = 0.2116.

The TSH response to diet-induced hypothyroidism is blunted in *Igsf1*$^{\Delta 312/y}$ mice

Though *Igsf1*$^{\Delta 312/y}$ males demonstrated a clear impairment in pituitary TSH synthesis, they were nonetheless able to attain a euthyroid state under normal laboratory conditions. We next asked how they would respond to a physiological challenge. Specifically, we rendered mice profoundly hypothyroid by placing them on a diet low in iodine and supplemented with propylthiouracil (LoI/PTU) for a period of 3 weeks. Serum TSH levels increased markedly across the 3 weeks of the experiment, from 1,090 to 63,640 pg/ml (Fig. 2.9A) in wild-type mice. TSH levels also increased in *Igsf1*$^{\Delta 312/y}$ mice, but the response was significantly blunted, from 964.1 pg/ml to 23,365 pg/ml (Fig. 2.9A). Serum T4 levels were significantly reduced within 1 week and maximally by 2 weeks for both genotypes (Fig. 2.9B). *Tshb*, *Cga*, and *Trhr* mRNA levels were also reduced in pituitaries of *Igsf1*$^{\Delta 312/y}$ males relative to controls after 3 weeks on the LoI/PTU diet (Fig. 2.9C-E).

TRH-induced TSH release is blunted in *Igsf1*$^{\Delta 312/y}$ mice

As *Igsf1* is expressed in both the brain and pituitary (59, 69-71), blunted TSH responses of *Igsf1*$^{\Delta 312/y}$ mice to the LoI/PTU diet could be explained by dysfunction in the hypothalamus, pituitary, or both. Though it is challenging to measure TRH directly in murine pituitary portal vessels, preliminary data from *Igsf1*$^{\Delta ex1/y}$ mice argue against a hypothalamic lesion. Specifically, *Trh* mRNA expression in the PVN is equivalent in wild-type and *Igsf1*$^{\Delta ex1/y}$ males on the LoI/PTU diet (T. Silander, unpublished). Moreover, *Trh* mRNA was appropriately downregulated when these mice were treated with exogenous T3 or T4 (T. Silander, unpublished), suggesting that TH feedback is normal at the level of the PVN.

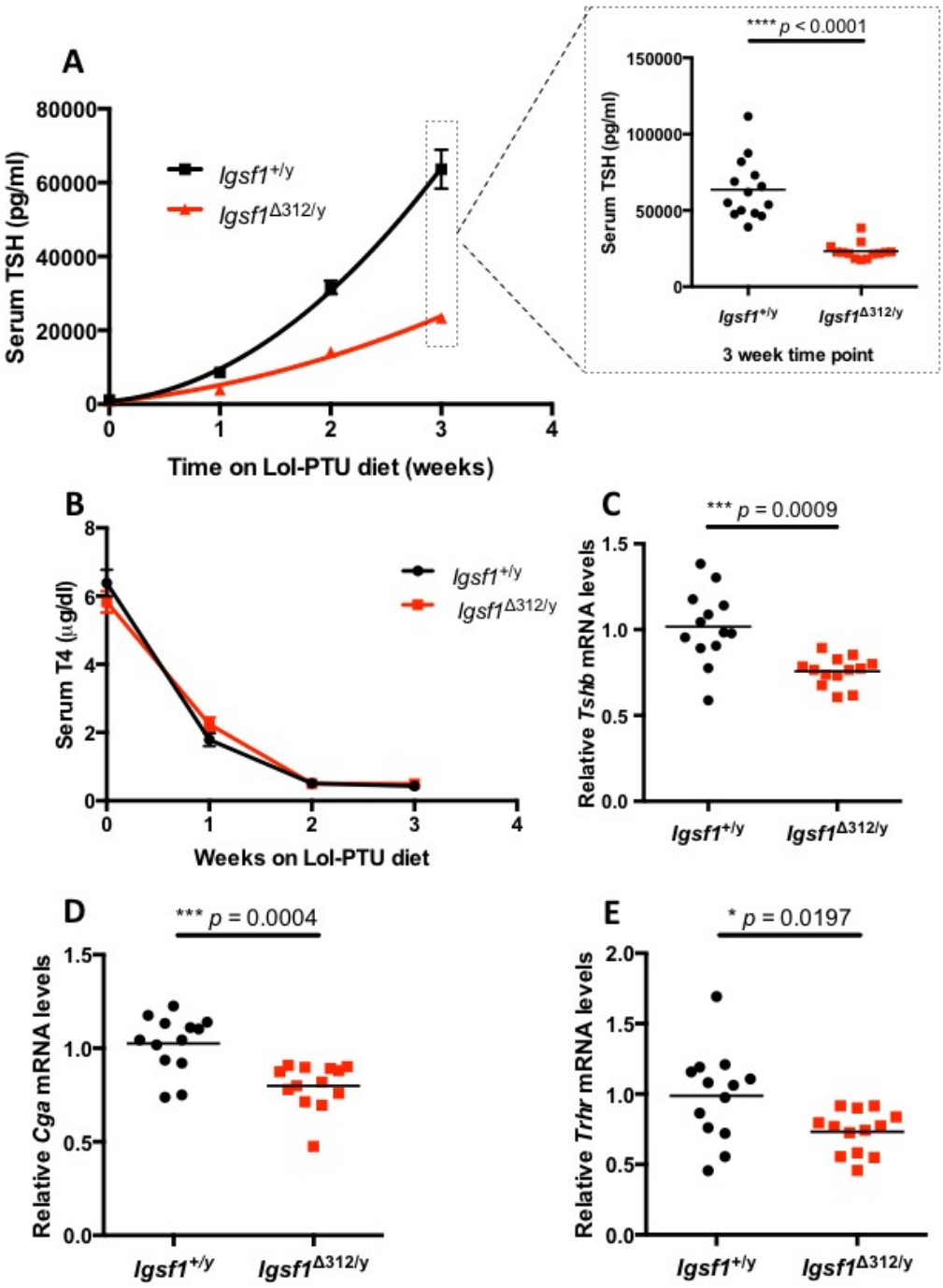

Figure 2.9 TSH release is blunted in *Igsf1*$^{\Delta 312}$ mice. Ten week-old male wild-type (black line) and *Igsf1*$^{\Delta 312/y}$ (red line) mice were placed on a LoI/PTU diet for 3 weeks. A) Serum TSH was measured immediately before, and then at weekly intervals after mice were placed on the diet. The data were analyzed by hybrid 2-way ANOVA (interaction: $F(3, 75) = 40.6$, **** $p < 0.0001$; time on diet: $F(3, 75) = 184.0$, **** $p < 0.0001$; genotype: $F(1, 25) = 77.68$, **** $p < 0.0001$) and post-hoc t-tests. n = 14 for wild-type and n = 13 for *Igsf1*$^{\Delta 312/y}$. Data at the three week time point are expanded to show individual data points (two-tailed t-test: $t = 7.322$, $df = 15.16$, **** $p < 0.0001$). B) Serum T4 levels were measured from the same serum samples as in (A). The data were analyzed by 2-way ANOVA (interaction: $F(3, 97) = 2.148$, N.S. $p = 0.0992$; time on diet: $F(3, 97) = 349.2$, **** $p < 0.0001$; genotype: $F(1, 97) = 0.004213$, N.S. $p = 0.9484$). C-E) Pituitary RNA from the same animals as in (A) was extracted at 3 weeks and *Tshb*, *Cga,* and *Trhr* mRNA levels measured by qPCR. The data were analyzed by two-tailed t-tests, C) $t = 4.108$, $df = 15.71$, *** $p = 0.0009$, D) $t = 4.183$, $df = 22.89$, *** $p = 0.0004$, E) $t = 2.574$, $df = 17.07$, * $p = 0.0197$.

We therefore focused on pituitary responsiveness to TRH, in particular because of the reduced *Trhr* mRNA expression in both *Igsf1*$^{\Delta 312/y}$ (e.g., Fig. 2.7C) and *Igsf1*$^{\Delta ex1/y}$ mice (59). In response to exogenous TRH, wild-type males showed a robust increase in TSH secretion (from 413.5 to 6,461 pg/ml) within 15 min (Fig. 2.10). Plasma TSH levels were still elevated, but well below peak, after 1 h (836.1 pg/ml), and returned to baseline 2 h after TRH injection (358.5 pg/ml). The TSH response in *Igsf1*$^{\Delta 312/y}$ mice was comparatively blunted (368.6 to 2,770 pg/ml) 15 min after TRH injection (Fig. 2.10). We observed a similar impairment in TRH-induced TSH release in *Igsf1*$^{\Delta ex1/y}$ mice compared to *Igsf1*$^{+/y}$ littermates (T. Silander, unpublished).

Though TSH protein content is reduced in pituitaries of *Igsf1*$^{\Delta 312/y}$ (Fig. 2.8A) and *Igsf1*$^{\Delta ex1/y}$ mice (59), the extent of the blunted TRH response suggested reduced pituitary sensitivity to the ligand, and not simply that there was less TSH available to be released. Consistent with this idea, *Igsf1*-deficient mice exhibited impaired *Trhr* mRNA expression (Fig. 2.7C) (59). To address TRH responsiveness more directly, we examined induction of the immediate early gene, c-Fos, in thyrotropes of *Igsf1*$^{\Delta 312/y}$ and wild-type littermates (Fig. 2.11). The number of TSHβ^{+} cells was equivalent between the *Igsf1*$^{\Delta 312/y}$ and *Igsf1*$^{+/y}$ mice (Fig. 2.12A). Next we counted the TSHβ^{+}/c-Fos^{+} cells in pituitary sections 30 min following TRH or PBS injections. We saw a clear activation of c-Fos in thyrotrope cells of mice injected with TRH compared to controls injected with PBS (Fig. 2.11 and 2.12B). However, we did not see a statistical difference between the amount of activated thyrotropes in *Igsf1*$^{\Delta 312/y}$ and *Igsf1*$^{+/y}$ mice (Fig 2.12B).

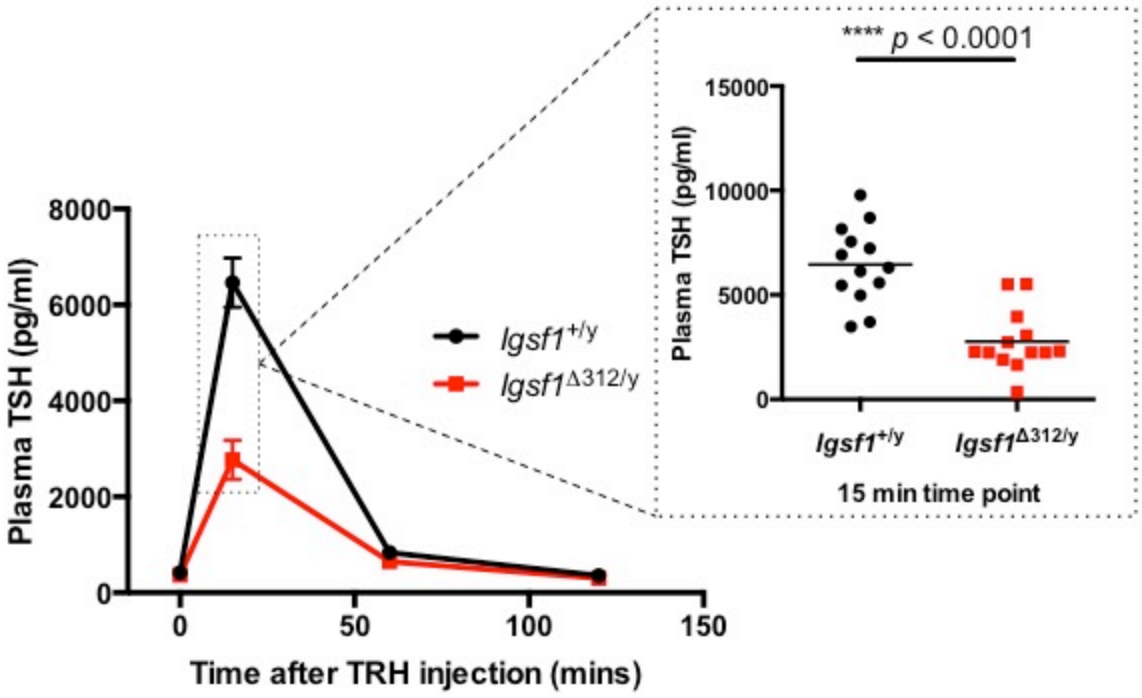

Figure 2.10 TRH induced TSH release is blunted in *Igsf1*$^{\Delta 312/y}$ mice. Eight week-old male wild-type and *Igsf1*$^{\Delta 312/y}$ mice were injected with TRH (i.p. 10 μ g/kg). Blood samples were collected before the TRH injection as well as 15 min, 1 h, and 2 h post-injection. Plasma TSH levels were measured by Luminex. Data were analyzed by 2-way ANOVA (interaction: $F(3, 99) = 30.31$, **** $p < 0.0001$; time after injection: $F(3, 99) = 160.9$, **** $p < 0.0001$; genotype: $F(1, 99) = 37.67$, **** $p < 0.0001$) and post-hoc t-test, n = 13 for each genotype. The data from the 15 min time point were expanded to show individual data points (two-tailed t-test: $t = 5.627$, $df = 22.72$, **** $p < 0.0001$).

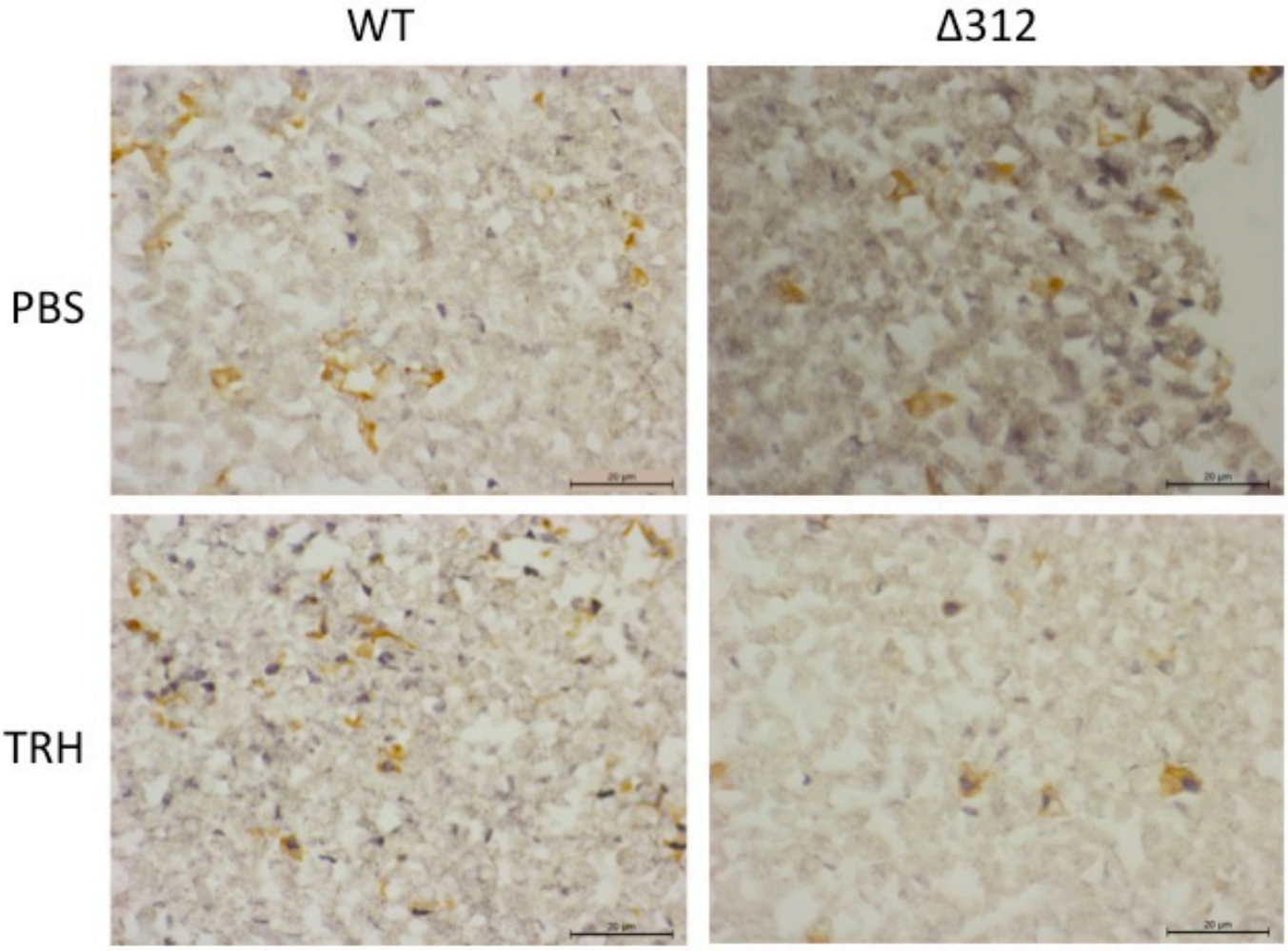

Figure 2.11 TRH-induced activation of TRHR in thyrotropes. Immunohistochemistry of fixed pituitaries from 8 week-old *Igsf1*$^{\Delta 312/y}$ (Δ 312) and *Igsf1*$^{+/y}$ (WT) mice injected with PBS or TRH 30 min prior to perfusion. TSH β^{+} cells are stained brown, and c-Fos^{+} cells have nuclei stained black.

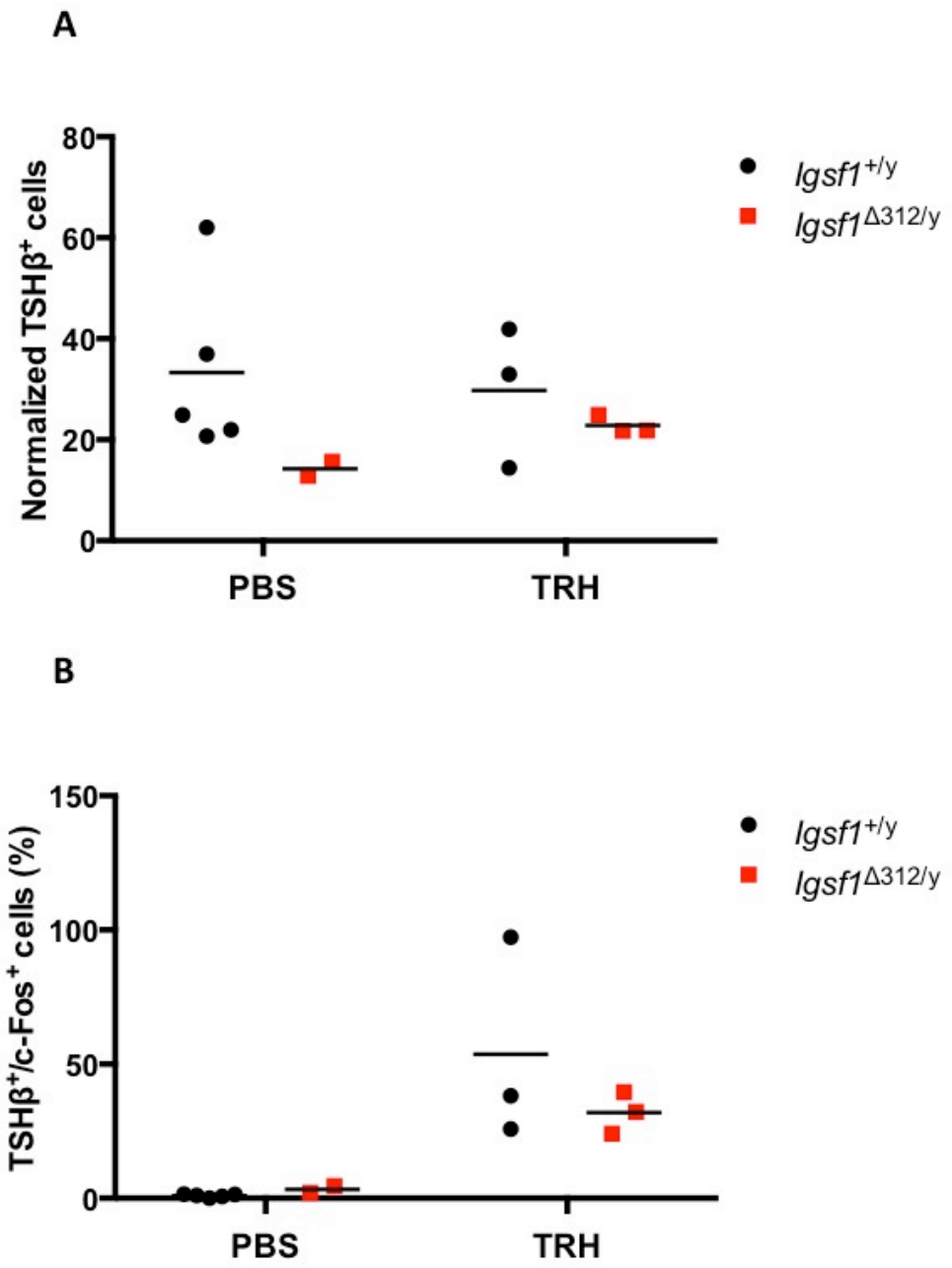

Figure 2.12 TRH-induced activation of TRHR in thyrotropes does not differ between *Igsf1*$^{\Delta 312/y}$ and *Igsf1*$^{+/y}$ mice. Quantification of TSH β^+ cells (A) and TSH β^+/c-Fos$^+$ cells (B) counted from stained pituitary sections. An example of the stained sections is shown in Figure 2.13. The data were analyzed by 2-way ANOVA. A) Interaction: F(1, 9) = 0.6087, N.S. $p = 0.4553$; treatment: F(1, 9) = 0.1056, N.S. $p = 0.7527$; genotype: F(1, 9) = 2.788, N.S. $p = 0.1293$. B) Interaction: F(1, 9) = 1.262, N.S. $p = 0.2904$; treatment: F(1, 9) = 14.33, ** $p = 0.0043$; genotype: F(1, 9) = 0.8166, N.S. $p = 0.3897$.

Discussion

IGSF1 plays a fundamental role in regulation of the HPT axis. Its exact role, however, has not been clearly defined (59). In this thesis, using a novel mouse model, I show that *Igsf1*-deficiency causes an impairment in pituitary *Trhr* expression and TRH action. Therefore, deficits in TRH signaling in pituitary thyrotropes, in part or in whole, underlie central hypothyroidism in IGSF1-deficiency syndrome.

IGSF1-CTD expression and membrane trafficking are impaired in *Igsf1*$^{\Delta 312}$ mice

The majority of *IGSF1* mutations in humans impair cell surface expression of the C-terminal domain (CTD) of the protein (59, 61, 63, 72, 76, 79). Similarly, the mice described here, with a 312 bp deletion in part of exon 18 and intron 18 of the *Igsf1* gene, have impaired IGSF1-CTD trafficking. Initially, we predicted that the trafficking defects in humans and mice were caused by the misfolding and/or incomplete glycosylation of the protein. However, with a single exception (in Ig loop 6), glycosylation of individual asparagine residues in the IGSF1-CTD is not required for membrane trafficking (B. Bak, unpublished). Therefore, the loss of two glycosylation sites in Ig loop 12 is unlikely to explain the trafficking defect in our mice. In all likelihood, the protein is misfolded, though we did not examine this directly (e.g., by limited proteolysis). It is also possible that the loss of the transmembrane domain and/or the C-terminal tail (C-tail) contributes to the trafficking defect. Our preliminary data indicate that trimming the C-tail to within 4 amino acids of the transmembrane domain impairs plasma membrane trafficking (M.O. Turgeon, unpublished).

The accumulation of misfolded IGSF1 proteins in the ER may cause ER stress. ER stress, in turn, can damage cells (80) and, therefore, impair functioning of cells

expressing mutant proteins. Nevertheless, we do not think that ER stress explains the central hypothyroidism phenotype in mice and humans with *Igsf1/IGSF1* mutations as patients with whole *IGSF1* gene deletion also exhibit CH (76). Therefore, it is most likely the loss of IGSF1-CTD function at the plasma membrane of pituitary thyrotrope cells that leads to CH.

Phenotypes in *Igsf1*$^{\Delta 312}$ derive from the on-target effect of Cas9

Our new *Igsf1*$^{\Delta 312}$ mouse model largely (though not identically) phenocopies both IGSF1 deficient patients and the previously described *Igsf1*$^{\Delta ex1}$ mouse model. The close correspondence in the phenotypes of the two mouse models suggests that: 1) there is little to no residual IGSF1-CTD in *Igsf1*$^{\Delta ex1}$ mice, and 2) loss of IGSF1-CTD function, and not off-target effects of Cas9, cause CH in the *Igsf1*$^{\Delta 312}$ mice. *Igsf1*$^{\Delta ex1}$ mice express an mRNA isoform that encodes the entirety of IGSF1-CTD. It was therefore possible that there might be partial compensation for the loss of the more abundant mRNA isoform 1 in these mice. The data here diminish this concern and further support the proposition that mRNA isoform 4 is likely vestigial and does not contribute to normal physiology, at least in the pituitary. With respect to the second point, there are diverging opinions about the likelihood of off-target effects occurring in animal models generated using CRISPR/Cas9 technology (81-83). Not only did our analysis fail to demonstrate off-target Cas9 activity (Fig. 2.6), the similarities between *Igsf1*$^{\Delta 312}$ and *Igsf1*$^{\Delta ex1}$ mice indicate that the critical mutation was in *Igsf1*, as designed.

Differences between *Igsf1*$^{\Delta 312}$ and *Igsf1*$^{\Delta ex1}$ mice

While the phenotypes of *Igsf1*$^{\Delta 312}$ and *Igsf1*$^{\Delta ex1}$ mice are highly similar, they are not identical. As described above, *Igsf1*$^{\Delta ex1}$ mice still express *Igsf1* mRNA isoform 4, but

lack the other 3 murine pituitary *Igsf1* isoforms (69). In contrast, we predict (but did not examine) that *Igsf1*$^{\Delta 312}$ mice will continue to express *Igsf1* mRNA isoforms 2 and 3 in their entirety, despite the demonstrated perturbation in their IGSF1-CTD expression, whether encoded by isoforms 1 or 4. Both models show decreased pituitary *Trhr* mRNA levels and TSH content. However, the models differ in that pituitary *Tshb* and *Cga* mRNA levels are reduced in *Igsf1*$^{\Delta 312}$ but not *Igsf1*$^{\Delta ex1}$ mice (59). Additionally, serum TSH and T4 levels appear normal in *Igsf1*$^{\Delta 312}$ mice on normal chow, but are reduced or normal in different cohorts of *Igsf1*$^{\Delta ex1}$ mice (59) (T. Silander, unpublished). We have not yet measured T3 in *Igsf1*$^{\Delta 312}$ mice, precluding a comparison of this hormone between the two models at this stage. Therefore, it is clear that in both cases, the animals show evidence of CH, but it is manifested in different ways for reasons we do not currently understand. There are additional differences between the two mouse models outside of the HPT axis. *Igsf1*$^{\Delta ex1}$ mice show increased pituitary GH content with normal *Gh* mRNA levels (B. Bak, unpublished), while *Igsf1*$^{\Delta 312}$ mice have increased *Gh* mRNA levels with normal GH pituitary content (Fig. 2.7 and 2.8). Also, *Igsf1*$^{\Delta 312}$ mice show increased testis weight while this characteristic is normal in *Igsf1*$^{\Delta ex1}$ mice. Whereas we are convinced that the IGSF1-CTD is abolished in both models, we cannot yet rule in or out modulatory roles for the other isoforms (in particular isoform 2), which are present in one model and absent in the other.

TRH action is impaired in *Igsf1*$^{\Delta 312}$ mice

Pituitary *Trhr* mRNA levels are reduced in both *Igsf1*-deficient mouse models. This suggests that: 1) IGSF1 somehow regulates expression of the gene (more below), and 2) impairments in TRH action in thyrotropes might underlie CH in these animals and

in patients. Indeed, we previously reported that IGSF1-deficient individuals show reduced TSH release in response to exogenous TRH (59, 60). Here, we similarly observed blunted TSH release in *Igsf1*$^{\Delta 312/y}$ mice compared to wild-type littermates. The same holds true for *Igsf1*$^{\Delta ex1}$ mice (B. Bak and T. Silander, unpublished). When increasing endogenous TRH release by rendering the mice hypothyroid with a LoI/PTU diet, we again observed a dramatic impairment in TSH release in the *Igsf1*$^{\Delta 312}$ and *Igsf1*$^{\Delta ex1}$ mice. Collectively, these data demonstrate impaired TRH action in thyrotrope cells.

However, the data does not allow us to differentiate between a few non-mutually exclusive explanations for the impairment: 1) a reduction in TRHR protein expression in thyrotropes, 2) a signaling defect downstream of TRHR, or 3) a reduction in the releasable pool of pituitary TSH. It seems likely that the TRHR protein is also reduced, though we did not measure this directly. It is also clear that pituitary TSH content is reduced in both *Igsf1*-deficient models. However, the extent of this reduction (24% lower in *Igsf1*$^{\Delta 312}$ mice) does not fully account for the degree to which TRH-induced TSH release is blunted (58% lower in *Igsf1*$^{\Delta 312}$ mice). Thus, we speculate that reduced TRHR levels lead to reduced thyrotrope sensitivity to TRH. We cannot presently rule out impairments in downstream signaling, but we have no data physically or functionally linking IGSF1 to TRHR. That is, we do not yet know if or how IGSF1 signals, and IGSF1 and TRHR do not physically interact (B. Bak, unpublished).

It is also possible that loss of IGSF1 affects thyrotrope development since IGSF1 is expressed in Rathke's pouch (59). Therefore, reductions in *Tshb*, *Cga*, and *Trhr* mRNA levels as well as TSH protein content could reflect reduced numbers of thyrotropes.

However, we did not observe statistically significant differences in the numbers of thyrotropes between genotypes. Thus, impaired TRHR expression/signaling remains the most parsimonious explanation for the observed pituitary phenotypes.

IGSF1-regulated TRHR levels modulate the response to environmental stimuli

The HPT axis is equipped to respond to various environmental stimuli including: cold, starvation, exercise, stress, and circadian rhythms (2, 84, 85). These stimuli can either activate or repress the activity of the axis. Our data suggest that IGSF1 may be most relevant in the context of stimulatory factors. However, this does not mean that IGSF1 is a sensor of stimuli, especially since *Trhr* expression is already low in *Igsf1*$^{\Delta 312}$ mice on a normal diet (Fig. 2.7C). Rather, as mentioned above, we hypothesize that IGSF1 regulates, directly or indirectly, the expression of TRHR, and that TRHR expression levels modulate the extent of the response to an HPT axis challenge. Therefore, under 'normal' conditions, TRHR expression in *Igsf1*$^{\Delta 312}$ mice is enough to achieve a sufficient TRH response that promotes normal circulating levels of TSH, and normal synthesis and secretion of THs, although the synthesis of the TSH subunits is down. However, we see a deficit when the system is challenged. The increased TRH stimulation that drives more TSH release cannot be sustained fully in the *Igsf1*$^{\Delta 312}$ mice with reduced TRHR expression. This hypothesis is supported by the blunted increase of TSH following TRH injection or the hypothyroid diet (Fig. 2.10).

The variable penetrance in humans and mice might, therefore, reflect differences in TRH drive between individuals. These could be chronic differences dictated by genetics/epigenetics, or they could be in response to acute environmental stimuli. While, theoretically, mice kept under standard laboratory conditions are exposed to the same

environmental conditions, some animals may, in fact, experience different stimulating factors (cold, stress) in practice. Similarly, humans are also exposed to different stimuli in their everyday lives, and, when sampled individually and at different times, may indicate such variations.

IGSF1's role(s) in the pituitary

While the exact function of IGSF1 is still unclear, our data demonstrate that it plays a role, directly or indirectly, in the regulation of *Trhr* expression. Unfortunately, mechanisms of *Trhr* regulation have not been studied extensively, particularly *in vivo*. *In vitro*, treatments of pituitary cell lines GH3 and GH4C1 with TRH leads to reduced *Trhr* mRNA levels, while treatments with THs do not cause any observable effects (86-88). However, there are discrepancies between these results and what has been observed *in vivo*, where removing thyroid hormones by thyroidectomy in rat results in increased *Trhr* mRNA levels (87). The results in rat suggest two non-mutually exclusive possibilities for the regulation of *Trhr*: 1) TRH upregulates *Trhr* expression, and/or 2) THs negatively regulate *Trhr* expression. However, our data demonstrate that these two potential regulatory mechanisms are not dependent on proper IGSF1 expression. *Igsf1*$^{\Delta ex1/y}$ mice on the LoI/PTU diet exhibit similar *Trh* mRNA levels as wild-type controls (T. Silander, unpublished), and *Igsf1*$^{\Delta 312}$ mice have no change in T4 levels while *Trhr* mRNA is affected (Fig. 2.6C and 2.7C). These data suggest that other IGSF1-dependent regulatory mechanisms for *Trhr* expression are involved in the pituitary.

Some of these mechanisms may be inferred from studying the predicted structure of IGSF1 and comparing it to other proteins with similar organization. For example, osteoclast-associated receptor (OSCAR) is formed of two Ig-loops, a transmembrane

domain, and a short C-tail (89). Just like IGSF1, OSCAR is also expressed at the cell surface and contains a positively charged amino acid in its transmembrane domain (89). This charged amino acid allows OSCAR to interact with an immunoreceptor tyrosine-based activation motif (ITAM) containing protein. OSCAR interacts with the intracellular protein Fc receptor common γ (FcRγ) (90) which signals through phosphorylation of the tyrosine residues contained in its ITAM (91). This activation leads to increased intracellular calcium, and cytokines and chemokine production (92). OSCAR signaling is activated upon binding to collagen I, II , and III (90, 93). Since OSCAR and IGSF1 share a similar organization, we hypothesize that IGSF1 may transmit extracellular information into the cell via a mechanism similar to OSCAR, which relies on an ITAM-containing intracellular protein. This signaling pathway could then lead to the regulation of *Trhr* mRNA, just like OSCAR leads to gene expression changes (92, 94). Since OSCAR and other Ig-loop containing proteins (95) bind extracellular matrix, IGSF1 may function similarly, and, therefore, provide information to the cell about its extracellular environment.

Effects of the *Igsf1*$^{\Delta 312}$ mutation on other pituitary cell types

In addition to thyrotropes, *Igsf1* is produced in other TRHR-expressing cell types, somatotropes and lactotropes (59). Consistent with this pattern of expression, patients with IGSF1 deficiency present with variable hypoprolactinemia and growth hormone deficiency (57-59, 72, 76, 77, 79, 96). *Igsf1*$^{\Delta 312}$ mice have increased pituitary *Gh* mRNA levels and body mass relative to controls. *Prl* mRNA levels did not differ between genotypes. It is not yet clear whether the altered *Gh* expression reflects changes in TRHR expression or function in somatotropes. As *Trhr* is expressed in thyrotropes,

somatotropes, and lactotropes, but thyrotropes are a minority cell population (97-99), it seems likely that the receptor expression is reduced in all three cell types. While the physiological role of TRH in regulating GH is still unclear, exogenous TRH increases circulating GH levels in different animals, including rodents and humans (100). TRH can bind directly to somatotropes and regulate GH (101), in which case a TRHR decrease would lead to reduced GH. However, there are other indirect ways by which TRH can regulate GH. For example, the thyroid hormone status of rats has an impact on the TRH-induced GH response (102), and it has been proposed that there are other neuromodulatory effects of TRH that could lead to increased GH (100). Therefore, it is possible that decreased TRHR expression in the pituitary of *Igsf1/IGSF1* deficient mice and humans affect GH levels. However, given that GH is increased in mice and variably decreased in humans, we hypothesize that other species-specific indirect roles of IGSF1 or the HPT axis might modulate GH levels.

Extra-pituitary roles for IGSF1

While the above discussion pertains to a defect due to a loss-of-function of IGSF1 at the level of the pituitary, we also need to consider potential effects at different levels of the HPT axis. In particular, IGSF1 is expressed in the hypothalamus and in the choroid plexus, suggesting a potential role for the protein in TH feedback. We initially reported that *Trh* mRNA levels are lower in *Igsf1*$^{\Delta ex1/y}$ mice compared to wild-type littermates (59). However, this was most likely caused by a loss of TH feedback as this initial cohort of mice showed decreased T3 levels (59). In the following analysis with mice on a LoI/PTU diet, there were no differences in *Trh* mRNA levels. This does not, however, exclude the possibility that there is a change in the secretion of TRH into the pituitary

portal vessels. Nonetheless, *Trh* mRNA levels in the PVN are reduced equivalently in response to T3 or T4 in *Igsf1*$^{\Delta ex1}$ and control mice on a LoI/PTU diet (T. Silander, unpublished). These data suggest that feedback mechanisms in the brain are intact in *Igsf1*-deficient mice.

IGSF1 is also expressed in human and rat testes, but it has not been detected in murine testis (59, 70). It should be noted that both IGSF1 deficient mouse models as well as humans are fertile, but we have yet to collect sperm count data. *IGSF1* mutations in humans cause macroochidism (enlarged testes), and *Igsf1*$^{\Delta 312/y}$ mice also show increased testicular weight. Interestingly, however, the *Igsf1*$^{\Delta ex1}$ mice do not have increased testis mass. The fact that enlarged testes are observed in both humans and *Igsf1*$^{\Delta 312/y}$ mice, while only the former express IGSF1 in their testes, points to an indirect effect rather than a local IGSF1 defect. Testis weight is influenced mostly by the amount of spermatocytes, which is ultimately regulated by the Sertoli cells that are necessary for proper production of sperm (103). THs are important for the maturation of Sertoli cells. That is, THs are important for Sertoli cells to switch from a proliferative status into a spermatogenesis status (104). Therefore, hypothyroidism in neonatal animals leads to a delayed maturation of Sertoli cells, which allows them to proliferate further (104, 105). If the thyroid status is restored to normal during adulthood, there is a higher number of Sertoli cells present which leads to increased sperm production and enlarged testes (104, 106). As such, IGSF1-deficient mice and humans may be hypothyroid in early neonatal development (which has yet to be tested), therefore leading to a larger number of Sertoli cells, and, thereby, enlarged testes, in adulthood after normal TH levels are restored.

Conclusion

The data presented in this thesis suggest a role for IGSF1 as a modulator of TRH action. However, more investigations are needed to elucidate how IGSF1 influences TRHR expression and/or signaling. Deciphering the function of IGSF1 will enrich current understanding of the complex functioning of the HPT axis, which is important for the regulation of a number of physiological functions. It will also help us to better understand the underlying causes of central hypothyroidism and other phenotypes in IGSF1-deficiency syndrome.

References

1. Tata JR, Ernster L, and Lindberg O. Control of basal metabolic rate by thyroid hormones and cellular function. *Nature.* 1962;193(1058-60.

2. Joseph-Bravo P, Jaimes-Hoy L, Uribe RM, and Charli JL. 60 YEARS OF NEUROENDOCRINOLOGY: TRH, the first hypophysiotropic releasing hormone isolated: control of the pituitary-thyroid axis. *The Journal of endocrinology.* 2015;227(3):X3.

3. Boelen A, Wiersinga WM, and Fliers E. Fasting-induced changes in the hypothalamus-pituitary-thyroid axis. *Thyroid : official journal of the American Thyroid Association.* 2008;18(2):123-9.

4. Broeders EP, Vijgen GH, Havekes B, Bouvy ND, Mottaghy FM, Kars M, Schaper NC, Schrauwen P, Brans B, and van Marken Lichtenbelt WD. Thyroid Hormone Activates Brown Adipose Tissue and Increases Non-Shivering Thermogenesis--A Cohort Study in a Group of Thyroid Carcinoma Patients. *PloS one.* 2016;11(1):e0145049.

5. Patel J, Landers K, Li H, Mortimer RH, and Richard K. Thyroid hormones and fetal neurological development. *The Journal of endocrinology.* 2011;209(1):1-8.

6. Khandelwal D, and Tandon N. Overt and subclinical hypothyroidism: who to treat and how. *Drugs.* 2012;72(1):17-33.

7. Carle A, Pedersen IB, Knudsen N, Perrild H, Ovesen L, and Laurberg P. Gender differences in symptoms of hypothyroidism: a population-based DanThyr study. *Clinical endocrinology.* 2015;83(5):717-25.

8. Goichot B, Caron P, Landron F, and Bouee S. Clinical presentation of hyperthyroidism in a large representative sample of outpatients in France: relationships with age, aetiology and hormonal parameters. *Clinical endocrinology.* 2016;84(3):445-51.

9. Hokfelt T, Fuxe K, Johansson O, Jeffcoate S, and White N. Distribution of thyrotropin-releasing hormone (TRH) in the central nervous system as revealed with immunohistochemistry. *European journal of pharmacology.* 1975;34(2):389-92.

10. Lechan RM, and Jackson IM. Immunohistochemical localization of thyrotropin-releasing hormone in the rat hypothalamus and pituitary. *Endocrinology.* 1982;111(1):55-65.

11. Grant G, Vale W, and Guillemin R. Interaction of thyrotropin releasing factor with membrane receptors of pituitary cells. *Biochemical and biophysical research communications.* 1972;46(1):28-34.

12. Kourides IA, Weintraub BD, Ridgway EC, and Maloof F. Increase in the beta subunit of human TSH in hypothyroid serum after thyrotropin releasing hormone. *The Journal of clinical endocrinology and metabolism.* 1973;37(5):836-40.

13. Weintraub BD, Gesundheit N, Taylor T, and Gyves PW. Effect of TRH on TSH glycosylation and biological action. *Annals of the New York Academy of Sciences.* 1989;553(205-13.

14. Chiamolera MI, and Wondisford FE. Minireview: Thyrotropin-releasing hormone and the thyroid hormone feedback mechanism. *Endocrinology.* 2009;150(3):1091-6.

15. Larsen PR. Thyroid-pituitary interaction: feedback regulation of thyrotropin secretion by thyroid hormones. *The New England journal of medicine.* 1982;306(1):23-32.

16. Segerson TP, Kauer J, Wolfe HC, Mobtaker H, Wu P, Jackson IM, and Lechan RM. Thyroid hormone regulates TRH biosynthesis in the paraventricular nucleus of the rat hypothalamus. *Science.* 1987;238(4823):78-80.

17. Shupnik MA, Chin WW, Habener JF, and Ridgway EC. Transcriptional regulation of the thyrotropin subunit genes by thyroid hormone. *The Journal of biological chemistry.* 1985;260(5):2900-3.

18. Galton VA, de Waard E, Parlow AF, St Germain DL, and Hernandez A. Life without the iodothyronine deiodinases. *Endocrinology.* 2014;155(10):4081-7.

19. Gereben B, Zavacki AM, Ribich S, Kim BW, Huang SA, Simonides WS, Zeold A, and Bianco AC. Cellular and molecular basis of deiodinase-regulated thyroid hormone signaling. *Endocrine reviews.* 2008;29(7):898-938.

20. Gereben B, Zeold A, Dentice M, Salvatore D, and Bianco AC. Activation and inactivation of thyroid hormone by deiodinases: local action with general consequences. *Cellular and molecular life sciences : CMLS.* 2008;65(4):570-90.

21. Heuer H, and Visser TJ. The pathophysiological consequences of thyroid hormone transporter deficiencies: Insights from mouse models. *Biochimica et biophysica acta.* 2013;1830(7):3974-8.

22. Visser WE, Friesema EC, and Visser TJ. Minireview: thyroid hormone transporters: the knowns and the unknowns. *Molecular endocrinology.* 2011;25(1):1-14.

23. Chakera AJ, Pearce SH, and Vaidya B. Treatment for primary hypothyroidism: current approaches and future possibilities. *Drug design, development and therapy.* 2012;6(1-11.

24. Hetzel BS. Iodine deficiency disorders (IDD) and their eradication. *Lancet.* 1983;2(8359):1126-9.

25. Vanderpump MP. The epidemiology of thyroid disease. *British medical bulletin.* 2011;99(39-51.

26. Marians RC, Ng L, Blair HC, Unger P, Graves PN, and Davies TF. Defining thyrotropin-dependent and -independent steps of thyroid hormone synthesis by using thyrotropin receptor-null mice. *Proceedings of the National Academy of Sciences of the United States of America.* 2002;99(24):15776-81.

27. Visser TJ, and Peeters RP. In: De Groot LJ, Beck-Peccoz P, Chrousos G, Dungan K, Grossman A, Hershman JM, Koch C, McLachlan R, New M, Rebar R, et al. eds. *Endotext*. South Dartmouth (MA); 2000.

28. Deme D, Pommier J, and Nunez J. Specificity of thyroid hormone synthesis. The role of thyroid peroxidase. *Biochimica et biophysica acta.* 1978;540(1):73-82.

29. Avbelj M, Tahirovic H, Debeljak M, Kusekova M, Toromanovic A, Krzisnik C, and Battelino T. High prevalence of thyroid peroxidase gene mutations in patients with thyroid dyshormonogenesis. *European journal of endocrinology / European Federation of Endocrine Societies.* 2007;156(5):511-9.

30. Beamer WJ, Eicher EM, Maltais LJ, and Southard JL. Inherited primary hypothyroidism in mice. *Science.* 1981;212(4490):61-3.

31. Tenenbaum-Rakover Y, Grasberger H, Mamanasiri S, Ringkananont U, Montanelli L, Barkoff MS, Dahood AM, and Refetoff S. Loss-of-function mutations in the thyrotropin receptor gene as a major determinant of hyperthyrotropinemia in a consanguineous community. *The Journal of clinical endocrinology and metabolism.* 2009;94(5):1706-12.

32. Sunthornthepvarakui T, Gottschalk ME, Hayashi Y, and Refetoff S. Brief report: resistance to thyrotropin caused by mutations in the thyrotropin-receptor gene. *The New England journal of medicine.* 1995;332(3):155-60.

33. Hiromatsu Y, Satoh H, and Amino N. Hashimoto's thyroiditis: history and future outlook. *Hormones.* 2013;12(1):12-8.

34. Giordano C, Stassi G, De Maria R, Todaro M, Richiusa P, Papoff G, Ruberti G, Bagnasco M, Testi R, and Galluzzo A. Potential involvement of Fas and its ligand in the pathogenesis of Hashimoto's thyroiditis. *Science.* 1997;275(5302):960-3.

35. Menconi F, Monti MC, Greenberg DA, Oashi T, Osman R, Davies TF, Ban Y, Jacobson EM, Concepcion ES, Li CW, et al. Molecular amino acid signatures in the MHC class II peptide-binding pocket predispose to autoimmune thyroiditis in humans and in mice. *Proceedings of the National Academy of Sciences of the United States of America.* 2008;105(37):14034-9.

36. Lania A, Persani L, and Beck-Peccoz P. Central hypothyroidism. *Pituitary.* 2008;11(2):181-6.

37. Persani L. Clinical review: Central hypothyroidism: pathogenic, diagnostic, and therapeutic challenges. *The Journal of clinical endocrinology and metabolism.* 2012;97(9):3068-78.

38. Yamada M, and Mori M. Mechanisms related to the pathophysiology and management of central hypothyroidism. *Nature clinical practice Endocrinology & metabolism.* 2008;4(12):683-94.

39. Alatzoglou KS, and Dattani MT. Genetic forms of hypopituitarism and their manifestation in the neonatal period. *Early human development.* 2009;85(11):705-12.

40. Fang Q, Benedetti AF, Ma Q, Gregory L, Li JZ, Dattani M, Sadeghi-Nejad A, Arnhold IJ, de Mendonca BB, Camper SA, et al. HESX1 Mutations in Patients with Congenital Hypopituitarism: Variable Phenotypes with the Same Genotype. *Clinical endocrinology.* 2016.

41. Castinetti F, Reynaud R, Saveanu A, Jullien N, Quentien MH, Rochette C, Barlier A, Enjalbert A, and Brue T. MECHANISMS IN ENDOCRINOLOGY: An update in the genetic aetiologies of combined pituitary hormone deficiency. *European journal of endocrinology / European Federation of Endocrine Societies.* 2016;174(6):R239-47.

42. Bonomi M, Proverbio MC, Weber G, Chiumello G, Beck-Peccoz P, and Persani L. Hyperplastic pituitary gland, high serum glycoprotein hormone alpha-subunit, and variable circulating thyrotropin (TSH) levels as hallmark of central hypothyroidism due to mutations of the TSH beta gene. *The Journal of clinical endocrinology and metabolism.* 2001;86(4):1600-4.

43. McDermott MT, Haugen BR, Black JN, Wood WM, Gordon DF, and Ridgway EC. Congenital isolated central hypothyroidism caused by a "hot spot" mutation in the thyrotropin-beta gene. *Thyroid : official journal of the American Thyroid Association.* 2002;12(12):1141-6.

44. Dacou-Voutetakis C, Feltquate DM, Drakopoulou M, Kourides IA, and Dracopoli NC. Familial hypothyroidism caused by a nonsense mutation in the thyroid-

stimulating hormone beta-subunit gene. *American journal of human genetics.* 1990;46(5):988-93.

45. Koulouri O, Nicholas AK, Schoenmakers E, Mokrosinski J, Lane F, Cole T, Kirk J, Farooqi IS, Chatterjee VK, Gurnell M, et al. A Novel Thyrotropin-Releasing Hormone Receptor Missense Mutation (P81R) in Central Congenital Hypothyroidism. *The Journal of clinical endocrinology and metabolism.* 2016;101(3):847-51.

46. Sun Y, Lu X, and Gershengorn MC. Thyrotropin-releasing hormone receptors -- similarities and differences. *Journal of molecular endocrinology.* 2003;30(2):87-97.

47. Yu R, and Hinkle PM. Signal transduction and hormone-dependent internalization of the thyrotropin-releasing hormone receptor in cells lacking Gq and G11. *The Journal of biological chemistry.* 1999;274(22):15745-50.

48. Hsieh KP, and Martin TF. Thyrotropin-releasing hormone and gonadotropin-releasing hormone receptors activate phospholipase C by coupling to the guanosine triphosphate-binding proteins Gq and G11. *Molecular endocrinology.* 1992;6(10):1673-81.

49. Kiley SC, Parker PJ, Fabbro D, and Jaken S. Differential regulation of protein kinase C isozymes by thyrotropin-releasing hormone in GH4C1 cells. *The Journal of biological chemistry.* 1991;266(35):23761-8.

50. Shupnik MA, Weck J, and Hinkle PM. Thyrotropin (TSH)-releasing hormone stimulates TSH beta promoter activity by two distinct mechanisms involving calcium influx through L type Ca2+ channels and protein kinase C. *Molecular endocrinology.* 1996;10(1):90-9.

51. Ohmichi M, Sawada T, Kanda Y, Koike K, Hirota K, Miyake A, and Saltiel AR. Thyrotropin-releasing hormone stimulates MAP kinase activity in GH3 cells by divergent pathways. Evidence of a role for early tyrosine phosphorylation. *The Journal of biological chemistry.* 1994;269(5):3783-8.

52. Bonomi M, Busnelli M, Beck-Peccoz P, Costanzo D, Antonica F, Dolci C, Pilotta A, Buzi F, and Persani L. A family with complete resistance to thyrotropin-releasing hormone. *The New England journal of medicine.* 2009;360(7):731-4.

53. Collu R, Tang J, Castagne J, Lagace G, Masson N, Huot C, Deal C, Delvin E, Faccenda E, Eidne KA, et al. A novel mechanism for isolated central hypothyroidism: inactivating mutations in the thyrotropin-releasing hormone receptor gene. *The Journal of clinical endocrinology and metabolism.* 1997;82(5):1561-5.

54. Donadio S, Pascual A, Thijssen JH, and Ronin C. Feasibility study of new calibrators for thyroid-stimulating hormone (TSH) immunoprocedures based on remodeling of recombinant TSH to mimic glycoforms circulating in patients with thyroid disorders. *Clinical chemistry.* 2006;52(2):286-97.

55. Trojan J, Theodoropoulou M, Usadel KH, Stalla GK, and Schaaf L. Modulation of human thyrotropin oligosaccharide structures--enhanced proportion of sialylated and terminally galactosylated serum thyrotropin isoforms in subclinical and overt primary hypothyroidism. *The Journal of endocrinology.* 1998;158(3):359-65.

56. Rabeler R, Mittag J, Geffers L, Ruther U, Leitges M, Parlow AF, Visser TJ, and Bauer K. Generation of thyrotropin-releasing hormone receptor 1-deficient mice as an animal model of central hypothyroidism. *Molecular endocrinology.* 2004;18(6):1450-60.

57. Joustra SD, Schoenmakers N, Persani L, Campi I, Bonomi M, Radetti G, Beck-Peccoz P, Zhu H, Davis TM, Sun Y, et al. The IGSF1 deficiency syndrome: characteristics of male and female patients. *The Journal of clinical endocrinology and metabolism.* 2013;98(12):4942-52.

58. Joustra SD, van Trotsenburg AS, Sun Y, Losekoot M, Bernard DJ, Biermasz NR, Oostdijk W, and Wit JM. IGSF1 deficiency syndrome: A newly uncovered endocrinopathy. *Rare diseases.* 2013;1(e24883.

59. Sun Y, Bak B, Schoenmakers N, van Trotsenburg AS, Oostdijk W, Voshol P, Cambridge E, White JK, le Tissier P, Gharavy SN, et al. Loss-of-function mutations in IGSF1 cause an X-linked syndrome of central hypothyroidism and testicular enlargement. *Nature genetics.* 2012;44(12):1375-81.

60. Hughes JN, Aubert M, Heatlie J, Gardner A, Gecz J, Morgan T, Belsky J, and Thomas PQ. Identification of an IGSF1-specific deletion in a five generation pedigree with X-linked Central Hypothyroidism without macroorchidism. *Clinical endocrinology.* 2016.

61. Nakamura A, Bak B, Silander TL, Lam J, Hotsubo T, Yorifuji T, Ishizu K, Bernard DJ, and Tajima T. Three novel IGSF1 mutations in four Japanese patients with X-linked congenital central hypothyroidism. *The Journal of clinical endocrinology and metabolism.* 2013;98(10):E1682-91.

62. Hulle SV, Craen M, Callewaert B, Joustra S, Oostdijk W, Losekoot M, Wit JM, Turgeon MO, Bernard DJ, and Schepper JD. Delayed Adrenarche may be an Additional Feature of Immunoglobulin Super Family Member 1 Deficiency Syndrome. *Journal of clinical research in pediatric endocrinology.* 2016;8(1):86-91.

63. Rakover YT, Turgeon MO, London S, Hermanns P, Pohlenz J, Bernard DJ, and Bercovich D. Familial Central Hypothyroidism Caused by a Novel IGSF1 Gene Mutation. *Thyroid : official journal of the American Thyroid Association.* 2016.

64. Joustra SD, Heinen CA, Schoenmakers N, Bonomi M, Ballieux BE, Turgeon MO, Bernard DJ, Fliers E, van Trotsenburg AS, Losekoot M, et al. IGSF1 Deficiency: Lessons From an Extensive Case Series and Recommendations for Clinical Management. *The Journal of clinical endocrinology and metabolism.* 2016;101(4):1627-36.

65. Frattini A, Faranda S, Redolfi E, Allavena P, and Vezzoni P. Identification and genomic organization of a gene coding for a new member of the cell adhesion molecule family mapping to Xq25. *Gene.* 1998;214(1-2):1-6.

66. Mazzarella R, Pengue G, Jones J, Jones C, and Schlessinger D. Cloning and expression of an immunoglobulin superfamily gene (IGSF1) in Xq25. *Genomics.* 1998;48(2):157-62.

67. Robakis T, Bak B, Lin SH, Bernard DJ, and Scheiffele P. An internal signal sequence directs intramembrane proteolysis of a cellular immunoglobulin domain protein. *The Journal of biological chemistry.* 2008;283(52):36369-76.

68. Leshchyns'ka I, and Sytnyk V. Reciprocal Interactions between Cell Adhesion Molecules of the Immunoglobulin Superfamily and the Cytoskeleton in Neurons. *Frontiers in cell and developmental biology.* 2016;4(9.

69. Bernard DJ, Burns KH, Haupt B, Matzuk MM, and Woodruff TK. Normal reproductive function in InhBP/p120-deficient mice. *Molecular and cellular biology.* 2003;23(14):4882-91.

70. Joustra SD, Meijer OC, Heinen CA, Mol IM, Laghmani el H, Sengers RM, Carreno G, van Trotsenburg AS, Biermasz NR, Bernard DJ, et al. Spatial and temporal expression of immunoglobulin superfamily member 1 in the rat. *The Journal of endocrinology.* 2015;226(3):181-91.

71. Su AI, Wiltshire T, Batalov S, Lapp H, Ching KA, Block D, Zhang J, Soden R, Hayakawa M, Kreiman G, et al. A gene atlas of the mouse and human protein-encoding transcriptomes. *Proceedings of the National Academy of Sciences of the United States of America.* 2004;101(16):6062-7.

72. Joustra SD, Wehkalampi K, Oostdijk W, Biermasz NR, Howard S, Silander TL, Bernard DJ, Wit JM, Dunkel L, and Losekoot M. IGSF1 variants in boys with familial delayed puberty. *European journal of pediatrics.* 2015;174(5):687-92.

73. Livak KJ, and Schmittgen TD. Analysis of relative gene expression data using real-time quantitative PCR and the 2(-Delta Delta C(T)) Method. *Methods.* 2001;25(4):402-8.

74. Jinek M, Chylinski K, Fonfara I, Hauer M, Doudna JA, and Charpentier E. A programmable dual-RNA-guided DNA endonuclease in adaptive bacterial immunity. *Science.* 2012;337(6096):816-21.

75. Cong L, Ran FA, Cox D, Lin S, Barretto R, Habib N, Hsu PD, Wu X, Jiang W, Marraffini LA, et al. Multiplex genome engineering using CRISPR/Cas systems. *Science.* 2013;339(6121):819-23.

76. Joustra SD, Heinen CA, Schoenmakers N, Bonomi M, Ballieux BE, Turgeon MO, Bernard DJ, Fliers E, van Trotsenburg AS, Losekoot M, et al. IGSF1 deficiency: lessons from an extensive case series and recommendations for clinical management. *J Clin Endocrinol Metab.* 2016:jc20153880.

77. Tajima T, Nakamura A, and Ishizu K. A novel mutation of IGSF1 in a Japanese patient of congenital central hypothyroidism without macroorchidism. *Endocrine journal.* 2013;60(2):245-9.

78. Hsu PD, Scott DA, Weinstein JA, Ran FA, Konermann S, Agarwala V, Li Y, Fine EJ, Wu X, Shalem O, et al. DNA targeting specificity of RNA-guided Cas9 nucleases. *Nature biotechnology.* 2013;31(9):827-32.

79. Van Hulle S, Craen M, Callewaert B, Joustra SD, Oostdijk W, Losekoot M, Wit JM, Turgeon MO, Bernard D, and De Schepper J. Delayed Adrenarche May Be an Additional Feature of IGSF1 Deficiency Syndrome. *J Clin Res Pediatr Endocrinol.* 2015.

80. Sovolyova N, Healy S, Samali A, and Logue SE. Stressed to death - mechanisms of ER stress-induced cell death. *Biological chemistry.* 2014;395(1):1-13.

81. Fu Y, Foden JA, Khayter C, Maeder ML, Reyon D, Joung JK, and Sander JD. High-frequency off-target mutagenesis induced by CRISPR-Cas nucleases in human cells. *Nature biotechnology.* 2013;31(9):822-6.

82. Gabriel R, von Kalle C, and Schmidt M. Mapping the precision of genome editing. *Nature biotechnology.* 2015;33(2):150-2.

83. O'Geen H, Yu AS, and Segal DJ. How specific is CRISPR/Cas9 really? *Current opinion in chemical biology.* 2015;29(72-8.

84. Sotelo-Rivera I, Jaimes-Hoy L, Cote-Velez A, Espinoza-Ayala C, Charli JL, and Joseph-Bravo P. An acute injection of corticosterone increases thyrotrophin-releasing hormone expression in the paraventricular nucleus of the hypothalamus

but interferes with the rapid hypothalamus pituitary thyroid axis response to cold in male rats. *Journal of neuroendocrinology.* 2014;26(12):861-9.

85. Zoeller RT, Kabeer N, and Albers HE. Cold exposure elevates cellular levels of messenger ribonucleic acid encoding thyrotropin-releasing hormone in paraventricular nucleus despite elevated levels of thyroid hormones. *Endocrinology.* 1990;127(6):2955-62.

86. Gershengorn MC, and Osman R. Molecular and cellular biology of thyrotropin-releasing hormone receptors. *Physiological reviews.* 1996;76(1):175-91.

87. Yamada M, Monden T, Satoh T, Iizuka M, Murakami M, Iriuchijima T, and Mori M. Differential regulation of thyrotropin-releasing hormone receptor mRNA levels by thyroid hormone in vivo and in vitro (GH3 cells). *Biochemical and biophysical research communications.* 1992;184(1):367-72.

88. Oron Y, Straub RE, Traktman P, and Gershengorn MC. Decreased TRH receptor mRNA activity precedes homologous downregulation: assay in oocytes. *Science.* 1987;238(4832):1406-8.

89. Kim N, Takami M, Rho J, Josien R, and Choi Y. A novel member of the leukocyte receptor complex regulates osteoclast differentiation. *The Journal of experimental medicine.* 2002;195(2):201-9.

90. Barrow AD, Raynal N, Andersen TL, Slatter DA, Bihan D, Pugh N, Cella M, Kim T, Rho J, Negishi-Koga T, et al. OSCAR is a collagen receptor that costimulates osteoclastogenesis in DAP12-deficient humans and mice. *The Journal of clinical investigation.* 2011;121(9):3505-16.

91. Barrow AD, and Trowsdale J. You say ITAM and I say ITIM, let's call the whole thing off: the ambiguity of immunoreceptor signalling. *European journal of immunology.* 2006;36(7):1646-53.

92. Merck E, Gaillard C, Scuiller M, Scapini P, Cassatella MA, Trinchieri G, and Bates EE. Ligation of the FcR gamma chain-associated human osteoclast-associated receptor enhances the proinflammatory responses of human monocytes and neutrophils. *Journal of immunology.* 2006;176(5):3149-56.

93. Haywood J, Qi J, Chen CC, Lu G, Liu Y, Yan J, Shi Y, and Gao GF. Structural basis of collagen recognition by human osteoclast-associated receptor and design of osteoclastogenesis inhibitors. *Proceedings of the National Academy of Sciences of the United States of America.* 2016;113(4):1038-43.

94. Kim K, Kim JH, Lee J, Jin HM, Lee SH, Fisher DE, Kook H, Kim KK, Choi Y, and Kim N. Nuclear factor of activated T cells c1 induces osteoclast-associated receptor gene expression during tumor necrosis factor-related activation-induced

cytokine-mediated osteoclastogenesis. *The Journal of biological chemistry.* 2005;280(42):35209-16.

95. Barclay AN. Membrane proteins with immunoglobulin-like domains--a master superfamily of interaction molecules. *Seminars in immunology.* 2003;15(4):215-23.

96. Joustra SD, Roelfsema F, Endert E, Ballieux BE, van Trotsenburg AS, Fliers E, Corssmit EP, Bernard DJ, Oostdijk W, Wit JM, et al. Pituitary Hormone Secretion Profiles in IGSF1 Deficiency Syndrome. *Neuroendocrinology.* 2016;103(3-4):408-16.

97. Castrique E, Fernandez-Fuente M, Le Tissier P, Herman A, and Levy A. Use of a prolactin-Cre/ROSA-YFP transgenic mouse provides no evidence for lactotroph transdifferentiation after weaning, or increase in lactotroph/somatotroph proportion in lactation. *The Journal of endocrinology.* 2010;205(1):49-60.

98. Childs GV. Neonatal development of the thyrotrope in the male rat pituitary. *Endocrinology.* 1983;112(5):1647-52.

99. Galas L, Raoult E, Tonon MC, Okada R, Jenks BG, Castano JP, Kikuyama S, Malagon M, Roubos EW, and Vaudry H. TRH acts as a multifunctional hypophysiotropic factor in vertebrates. *General and comparative endocrinology.* 2009;164(1):40-50.

100. Harvey S. Thyrotrophin-releasing hormone: a growth hormone-releasing factor. *The Journal of endocrinology.* 1990;125(3):345-58.

101. Le Dafniet M, Garnier P, Bression D, Brandi AM, Racadot J, and Peillon F. Correlative studies between the presence of thyrotropin-releasing hormone (TRH) receptors and the in vitro stimulation of growth-hormone (GH) secretion in human GH-secreting adenomas. *Hormone and metabolic research = Hormon- und Stoffwechselforschung = Hormones et metabolisme.* 1985;17(9):476-9.

102. Chihara K, Kato Y, Ohgo S, Iwasaki Y, and Maeda K. Effects of hyperthyroidism and hypothyroidism on rat growth hormone release induced by thyrotropin-releasing hormone. *Endocrinology.* 1976;98(6):1396-400.

103. Orth JM, Gunsalus GL, and Lamperti AA. Evidence from Sertoli cell-depleted rats indicates that spermatid number in adults depends on numbers of Sertoli cells produced during perinatal development. *Endocrinology.* 1988;122(3):787-94.

104. De Franca LR, Hess RA, Cooke PS, and Russell LD. Neonatal hypothyroidism causes delayed Sertoli cell maturation in rats treated with propylthiouracil: evidence that the Sertoli cell controls testis growth. *The Anatomical record.* 1995;242(1):57-69.

105. Holsberger DR, Kiesewetter SE, and Cooke PS. Regulation of neonatal Sertoli cell development by thyroid hormone receptor alpha1. *Biology of reproduction.* 2005;73(3):396-403.

106. Cooke PS, and Meisami E. Early hypothyroidism in rats causes increased adult testis and reproductive organ size but does not change testosterone levels. *Endocrinology.* 1991;129(1):237-43.